TECHNOLOCY DEVELOPMENT FOR TRANSITION METAL-RARE EARTH HIGH-PERFORMANCE MAGNETIC MATERIALS

Contract No. F33615-70-C-1626
Sponsored by the Advanced Research Projects Agency
ARPA Order No. 1617, Program Code. No. OD10
Contract effective date: 30 June 1970. Expiration date: 30 June 1973

Approved for public release;
distribution unlimited.

Submitted to:

Air Force Materials Laboratory, AFSC, USAF
Project Engineer: J. C. Olson, LPE, Tel. (513) 255-4474

By:

J. J. Becker, Principal Investigator, Tel. (518) 346-8771, Ext. 6114
GENERAL ELECTRIC COMPANY
CORPORATE RESEARCH AND DEVELOPMENT
P. O. Box 8
SCHENECTADY, NEW YORK 12301

MISSING PAGE
NUMBERS ARE BLANK
AND WERE NOT
FILMED

NOTICE

When Government drawings, specifications, or other data are used for any purpose other than in connection with a definitely related Government procurement operation, the United States Government thereby incurs no responsibility nor any obligation whatsoever; and the fact that the government may have formulated, furnished, or in any way supplied the said drawings, specifications, or other data, is not to be regarded by implication or otherwise as in any manner licensing the holder or any other person or corporation, or conveying any rights or permission to manufacture, use, or sell any patented invention that may in any way be related thereto.

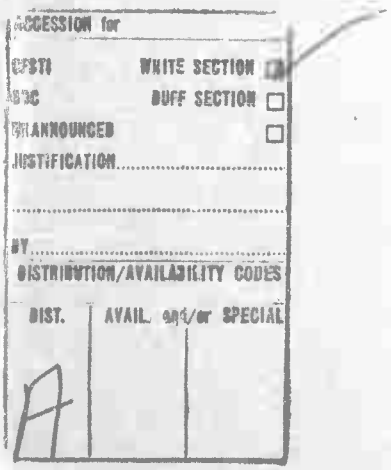

Copies of this report should not be returned unless return is required by security considerations, contractual obligations, or notice on a specific document.

UNCLASSIFIED

Security Classification

DOCUMENT CONTROL DATA - R & D

(Security classification of title, body of abstract and indexing annotation must be entered when the overall report is classified)

1. ORIGINATING ACTIVITY *(Corporate author)*
General Electric Company
Corporate Research and Development
Schenectady, New York

2a. REPORT SECURITY CLASSIFICATION
Unclassified

2b. GROUP

3. REPORT TITLE

TECHNOLOGY DEVELOPMENT FOR TRANSITION METAL-RARE EARTH HIGH-PERFORMANCE MAGNETIC MATERIALS

4. DESCRIPTIVE NOTES *(Type of report and inclusive dates)*
Semiannual Interim Technical Report July 1, 1971 to December 31, 1971

5. AUTHOR(S) *(First name, middle initial, last name)*

Joseph J. Becker

6. REPORT DATE	7a. TOTAL NO. OF PAGES	7b. NO. OF REFS
April 1972	41	38

8a. CONTRACT OR GRANT NO.	9a. ORIGINATOR'S REPORT NUMBER(S)
F-33615-70-C-1626	SRD-72-036
b. PROJECT NO. ARPA Order No. 1617	
c. Program Code No. OD10	9b. OTHER REPORT NO(S) *(Any other numbers that may be assigned this report)* AFML-TR-72-29
d.	

10. DISTRIBUTION STATEMENT

Approved for public release; distribution unlimited.

11. SUPPLEMENTARY NOTES	12. SPONSORING MILITARY ACTIVITY
	Air Force Materials Laboratory(LPE) Wright-Patterson Air Force Base Ohio 45433

13. ABSTRACT

In a Co_5Gd particle, a $1/\cos\theta$ angular dependence centering about an angle 28° from the alignment axis was observed for the field at which a magnetization jump took place. Analysis of the data indicates that the reversal was triggered by a bit of misoriented material pinning a wall fragment, and that the nucleus is very small and causes the jump to occur in the main body of the sample. It has been found that powders of Co_5Sm show great differences in their $H_c(H_m)$ curves at different T. For example, the H_c of a 50μ Co_5Sm powder in H_m of 44 kOe was more than three times as large at 77°K as at room T. This is in complete contrast to known data on the variation of K and M with T and indicates that the T dependence must be determined by the T variation of the relevant properties of the nucleation site, not those of the matrix. In a single particle, two magnetization discontinuities were followed as a function of temperature and it was found that their jumping fields H_n had different T dependences, strongly suggesting that they were of different natures. Domain structure observations as a function of thickness of a plane-parallel sample have permitted the evaluation of the wall energy of Co_5Sm at about 50 erg/cm^2. Observations of domain structure in $(Co, Fe)_{17}R_2$ materials have verified their easy-axis anisotropy. Comparison of wet analytical results from two sources show systematic discrepancies in the analyses of Co-Sm alloys. From a series of alloys made from a $Co_5Pr_{0.76}Sm_{0.24}$ base metal powder and a Co - 60 wt% additive powder, an alloy with a final nominal composition of 62.9 wt % Co, 21.3 wt % Pr, and 15.8 wt % Sm showed the following properties: B-coercive force, 10.1 kOe; $(BH)_{max}$, 26 mGOe. In view of the usual difficulty of attaining high coercivity in this class of alloys the above $_BH_c$ value is particularly noteworthy. A study has been made comparing the results of two approaches to the precise control of the composition of the sintered magnet necessary for high magnetic performance. These are 1) direct control of composition at the melting stage, and 2) control of composition by blending together powders of different compositions at a stage prior to alignment and densification. Although high performance magnets can be produced by either approach, one of the factors which lead to continued usage of the blending approach is the ability to optimize properties by making small shifts in composition at the powder stage.

DD FORM 1 NOV 68 1473

UNCLASSIFIED

Security Classification

14. KEY WORDS	LINK A		LINK B		LINK C	
	ROLE	WT	ROLE	WT	ROLE	WT
Magnetic Materials Permanent Magnets Cobalt-Rare Earth Magnetism						

TECHNOLOGY DEVELOPMENT FOR TRANSITION METAL-RARE EARTH HIGH-PERFORMANCE MAGNETIC MATERIALS

J. J. Becker

FOREWORD

This report describes work carried out in the Metallurgy and Ceramics Laboratory of the General Electric Research and Development Center, Schenectady, New York, under USAF Contract No. F33615-70-C-1626, entitled "Technology Development for Transition Metal-Rare Earth High-Performance Magnetic Materials." This work is administered by the Air Force Materials Laboratory, Wright-Patterson Air Force Base, Ohio, J. C. Olson (AFML/LPE), Project Engineer.

This Third Semiannual Interim Technical Report covers work conducted under the above program and related Company-funded programs during the period 1 July - 31 December 1971. The principal participants in the research are J. J. Becker, J. D. Livingston, J. G. Smeggil, R. J. Charles, D. L. Martin, L. Valentine, R. E. Cech, and M. G. Benz. The report was submitted by the author in January 1972.

The contractor's report number is SRD-72-036.

This technical report has been reviewed and is approved.

CHARLES E. EHRENFRIED
Major, USAF
Chief, Electromagnetic Materials Branch
Materials Physics Division
Air Force Materials Laboratory

ABSTRACT

In a Co_5Gd particle, a $1/\cos\theta$ angular dependence centering about an angle 28° from the alignment axis was observed for the field at which a magnetization jump took place. Analysis of the data indicates that the reversal was triggered by a bit of misoriented material pinning a wall fragment, and that the nucleus is very small and causes the jump to occur in the main body of the sample. It has been found that powders of Co_5Sm show great differences in their $H_c(H_m)$ curves at different T. For example, the H_c of a 50μ Co_5Sm powder in H_m of 44 kOe was more than three times as large at 77°K as at room T. This is in complete contrast to known data on the variation of K and M with T and indicates that the T dependence must be determined by the T variation of the relevant properties of the nucleation site, not those of the matrix. In a single particle, two magnetization discontinuities were followed as a function of temperature and it was found that their jumping fields H_n had different T dependences, strongly suggesting that they were of different natures. Domain structure observations as a function of thickness of a plane-parallel sample have permitted the evaluation of the wall energy of Co_5Sm at about 50 erg/cm^2. Observations of domain structure in $(Co, Fe)_{17}R_2$ materials have verified their easy-axis anisotropy. Comparison of wet analytical results from two sources shows systematic discrepancies in the analyses of Co-Sm alloys. From a series of alloys made from a $Co_5Pr_{0.76}Sm_{0.24}$ base metal powder and a Co - 60 wt % additive powder, an alloy with a final nominal composition of 62.9 wt % Co, 21.3 wt % Pr, and 15.8 wt % Sm showed the following properties: B-coercive force, 10.1 kOe; $(BH)_{max}$, 26 mGOe. In view of the usual difficulty of attaining high coercivity in this class of alloys the above $_BH_c$ value is particularly noteworthy. A study has been made comparing the results of two approaches to the precise control of the composition of the sintered magnet necessary for high magnetic performance. These are 1) direct control of composition at the melting stage, and 2) control of composition by blending together powders of different compositions at a stage prior to alignment and densification. Although high performance magnets can be produced by either approach, one of the factors which lead to continued usage of the blending approach is the ability to optimize properties by making small shifts in composition at the powder stage.

TABLE OF CONTENTS

LIST OF ILLUSTRATIONS

TECHNOLOGY DEVELOPMENT FOR TRANSITION METAL-RARE EARTH HIGH-PERFORMANCE MAGNETIC MATERIALS

J. J. Becker

I. INTRODUCTION

This is the third semiannual interim technical report for Contract No. F33615-70-C-1626, covering the period 1 July 1971 through 31 December 1971. The objective of this work, as set forth in Exhibit A of the contract, is to develop the technology of high-performance transition metal-rare earth magnets for critical applications. High-performance permanent magnets are defined in this context as those having remanences greater than ten thousand gauss and permeabilities of very nearly unity throughout the second and into the third quadrants of their hysteresis loop. Such technology is to be developed through 1) studies of the origin of the intrinsic coercive force in high-anisotropy materials, 2) development of information on phase equilibria in these systems, and 3) identification and investigation of new materials. The progress that has been made during the period covered by this report is described below under these three major headings.

II. FUNDAMENTAL STUDIES OF THE ORIGIN OF THE COERCIVE FORCE IN HIGH-ANISOTROPY MATERIALS

1. Angular Dependence of Nucleating Fields in Co-Rare Earth Particles (J. J. Becker)

(The text of the following section is identical with that of a paper that has been submitted for publication in the A. I. P. Conference Proceedings)

INTRODUCTION

The nature of the relationship of the coercive force to relevant structural features of cobalt-rare earth materials is not yet entirely clear. Co_5Sm seems consistently to yield much higher coercive forces for any type of treatment than other Co_5 (rare earth) or related compounds. On the other hand, the coercive forces attainable are still only a small fraction of the anisotropy field $2K/M_S$.

Vibrating-sample magnetometer measurements have shown[1] that single particles in the ~50μ size region show prominent discontinuities (jumps) in magnetization and may even reverse completely in one jump.[2] A more sensitive measuring technique has shown the same general behavior for still smaller particles.[3] It has been shown that each magnetization jump corresponds to the independent reversal of a portion of the particle.[4]

It seems clear that such behavior is to be interpreted not in classical

single-domain terms but as the result of domain boundary motion.[5] Boundaries can be nucleated or pinned by imperfections.[2, 3] In principle they can also be impeded by their inherent interaction with the crystal lattice,[6] but the importance of this effect at room temperature in these materials seems very doubtful.

The coercive force is then governed by imperfections, whose nature determines the fields at which domain boundary processes take place. Such imperfections could be of a number of types, somewhat as follows:

(1) Purely geometrical. M is uniform, but local fields are produced by the pole distributions on surface projections or indentations or internal voids or cracks. Nonmagnetic inclusions would be of this class, but there might be lattice strain associated with them as well.

(2) Lattice deformation. Elastic deformation, as around an inclusion, would add a local strain-magnetostriction anisotropy, whose magnitude would be unknown in these materials, in the absence of any information on their magnetostriction coefficients. Plastic deformation, as by mechanical processing, in which the lattice is disrupted, might well drastically affect the local anisotropy and perhaps also M.

(3) Composition variations. These can be inhomogeneities resulting from preparation, as for example from a peritectic reaction. They can result from local oxidation or volatilization of a component. They can also be associated with a discrete two-phase structure. In all cases the local M and K will gradually or suddenly change.

(4) Orientation variations. The local K axis may be displaced relative to the rest of the material either because of local deformation or because of the presence of a small grain of different orientation from the matrix.

Further information about their nature can be deduced in various ways. Direct visual observation of domains shows the sudden appearance of new reversed regions.[7] Etching experiments show that the particle surface can be an important site for imperfections.[1] The coercive force can be very sensitive to small amounts of strain.[8] Another way to infer information about the imperfections is to study the way in which the jump fields H_m depend on various parameters.

The parameter studied in this investigation was the angle at which the field H_n was applied. Different types of imperfections would be expected to have different angular dependences. In particular, if a jump were nucleated by a fragment of wall requiring a definite field H_n to bring it over some energy barrier, a $1/\cos\theta$ dependence would be expected, assuming that only 180° walls are present and that magnetization rotation is negligible. This is surely justifiable, as the H_n reported here are less than 1% of the anisotropy

field. Reich, Shtrikman, and Treves[9] have found a $1/\cos\theta$ angular dependence of the coercive force in orthoferrite single crystals, in which the reversal took place in a single jump, and concluded that "the coercive force is governed by the nucleation of a 180° domain wall." This can be understood if "nucleation" includes the initiation of the motion of a wall fragment already present.

EXPERIMENTAL RESULTS AND DISCUSSION

Measurements were made on a sample consisting of a roughly equiaxed particle of Co_5Gd approximately 500μ in average diameter. This particle was placed in the tip of a fine glass tube, in which it could move freely, with a small amount of paraffin. The tube was mounted in the sample holder of a vibrating-sample magnetometer. This sample holder was rotatable about the axis of vibration; that is, about an axis perpendicular to the field. With the sample holder set at 0°, the paraffin was melted, and then allowed to resolidify while a field of about 15 kOe was applied. Thus the orientation of the sample corresponding to $\theta = 0°$ was that which it spontaneously took up in the field. In this orientation, it showed pronounced and reproducible magnetization jumps like those that have been previously reported in other cobalt-rare earths.[1, 2, 3] The angular dependence of the jump field was then investigated.

For each value of θ at which measurements were made, the sample was first magnetized in a field H_m of 21 kOe at $\theta = 0°$. Then the field was reduced to zero, the sample rotated to the angle θ, and the magnetization as a function of increasing negative field recorded. Then the sample was returned to 0°, magnetized in 21 kOe in the opposite direction, and the opposite branch of the hysteresis loop similarly recorded. The hysteresis loop for $\theta = 0°$ is shown in Fig. 1. In this case, since the sample was not rotated, it was possible to record the magnetization in decreasing positive fields as well. In general this was not done.

Figure 1 shows one conspicuous magnetization jump at about 400 Oe, occurring on both sides of the hysteresis loop. The field at which this jump occurred was measured as a function of θ as described above. The jumps remained symmetrical about $H = 0$, and for each value of θ, both positive and negative values of the field H_n at which the jump occurred were recorded. This procedure was followed for both clockwise and counterclockwise rotations of the sample from the original magnetization direction. The results are shown in Fig. 2. Each experimental value represents from 6 to 24 observations and the error bars show ± one standard deviation.

It can be seen that the jump field follows an inverse cosine dependence quite well, but with a substantial angular offset. The dotted line in Fig. 2 is a plot of $H_n = 350/\cos(\theta + 28°)$ where θ is positive clockwise. This suggests that the nucleus for this jump is a small bit of material misoriented in such

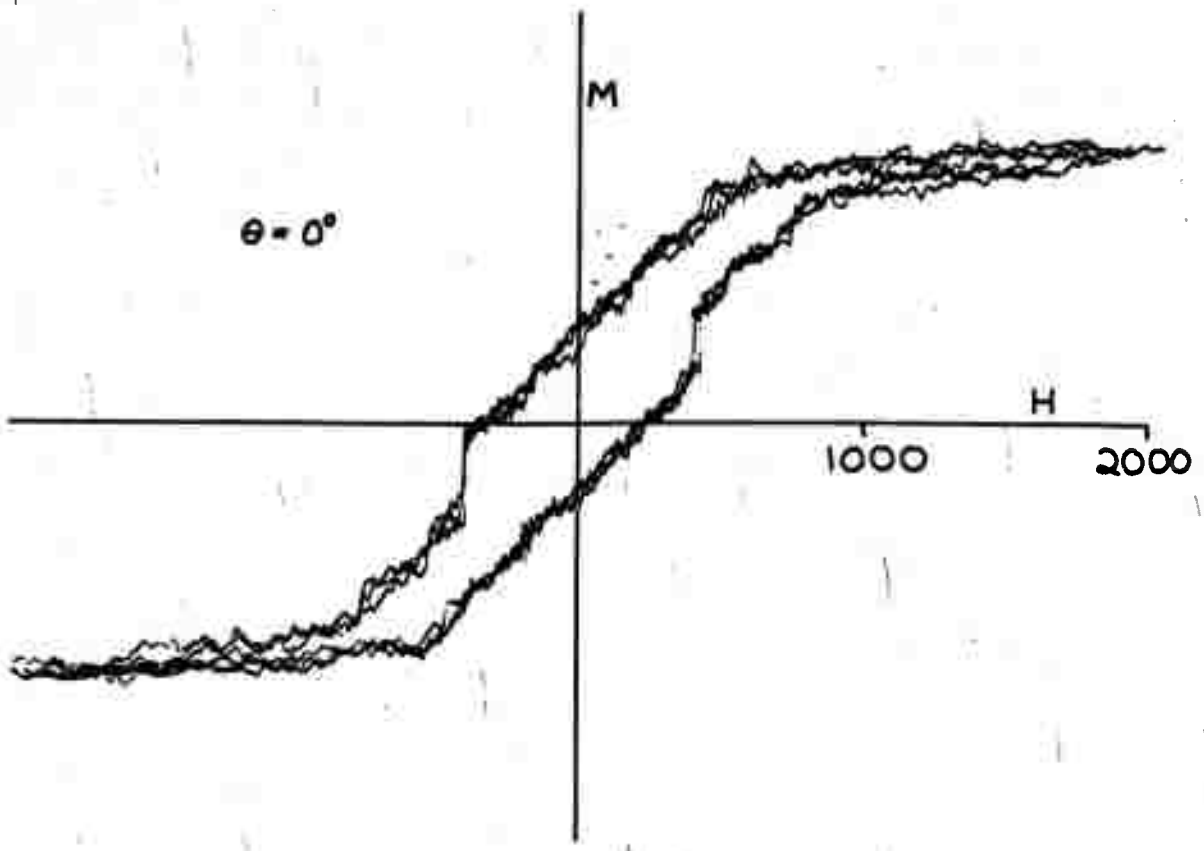

Figure 1 Hysteresis loop of ~500μ particle of Co_5Gd showing magnetization jumps. Traced three times. H_m = 21 kOe.

a way that the direction of its easy axis, projected on the plane of rotation, is 28° from that of the main body of the sample, and that it acts by trapping a fragment of wall within itself. This nucleus then triggers a reversal in the main body of the sample. This reversal does not go to completion, as has often been observed before.[4] The total magnetization change M, while not measured precisely, varied approximately as $\cos\theta$, not $\cos(\theta + 28°)$, eliminating the very unlikely possibility that the entire sample was misoriented 28° from the aligning field.

The question can then be raised: how can an off-orientation nucleus be distinguished from an off-orientation grain large enough so that its reversal would account for the entire magnetization jump? The jump gives about 12.8% of the total change in magnetization in Fig. 1. Such a change could conceivably, in the absence of positive structural information to the contrary, be caused by a secondary grain occupying 14% of the total volume and oriented in such a way that the projection of its easy axis on the plane of rotation is 32° from that of the main axis. This sample would align itself with the main

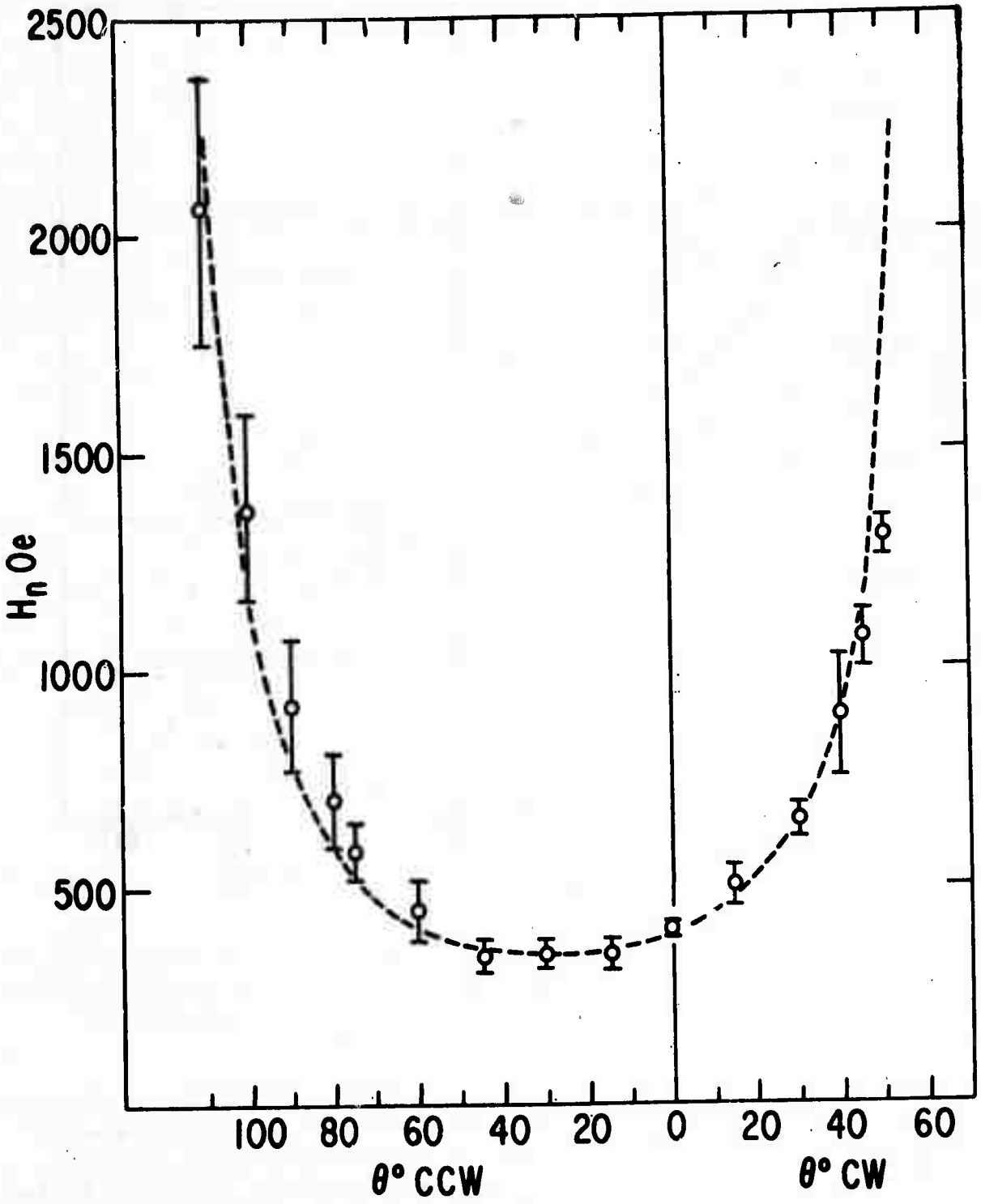

Figure 2 Jump field H_n as a function of angle θ for Co_5Gd particle shown in Fig. 1. Dotted line is $H_n = 350/\cos(\theta + 28°)$.

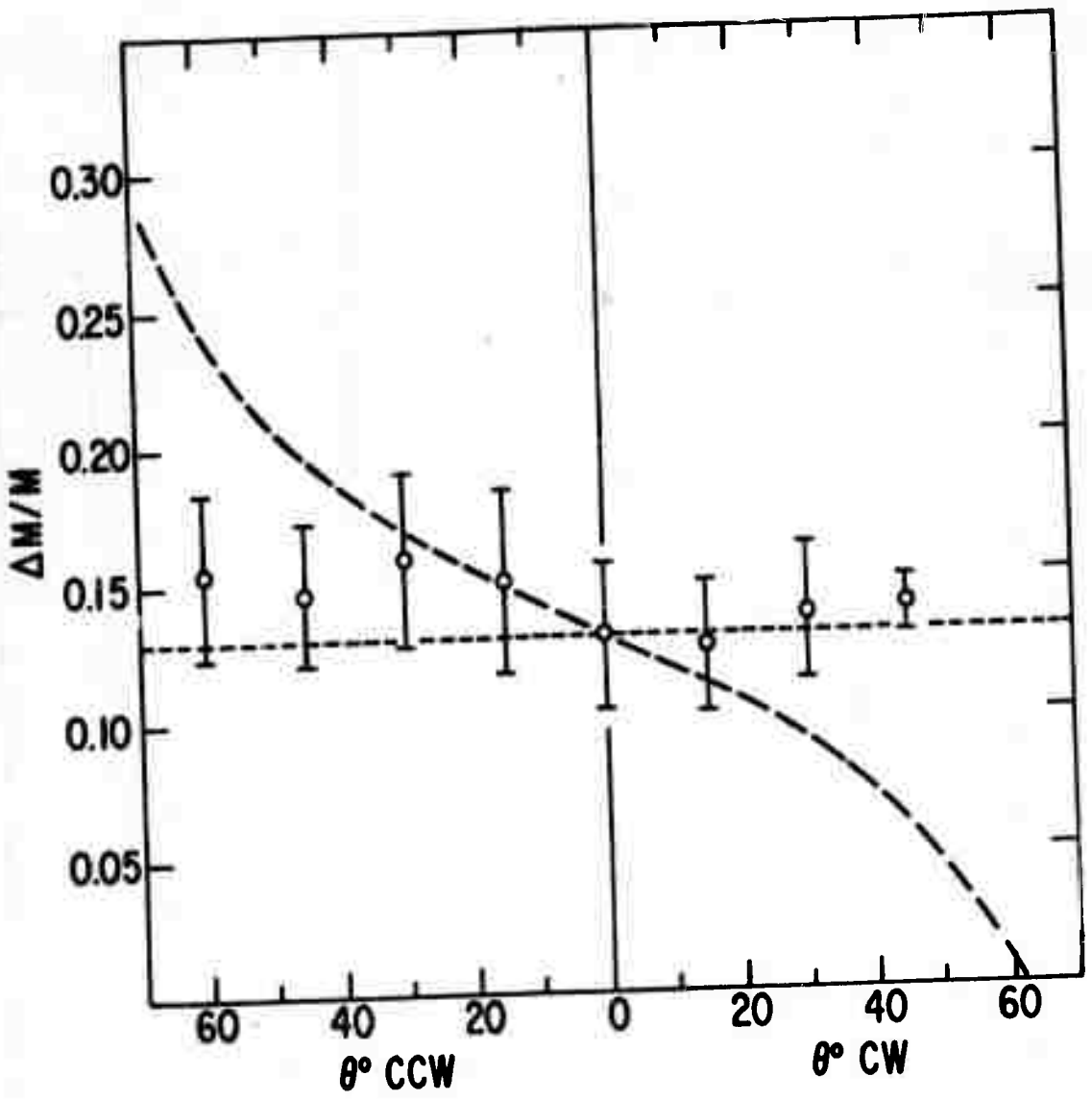

Figure 3 Fractional change in magnetization $\Delta M/M$ as a function of angle θ for Co_5Gd particle shown in Fig. 1. Horizontal dotted line is calculated for infinitesimally small nucleus, curved dashed line for secondary grain.

axis 4° from the direction of the aligning field and would give the angular dependence observed. However, these two possibilities can be distinguished by the behavior of the fractional change in magnetization due to the jump, $\Delta M/M$, with angle. For an infinitesimally small nucleus, $\Delta M/M$ will be the same for any θ, since both ΔM and M take place in the bulk of the material, and, being collinear, will have the same components at any angle. If ΔM occurs in a portion of the sample having a different orientation from the rest, the value of $\Delta M/M$ will range from zero, when the small grain is at 90° to the $\theta = 0$ axis, to infinity, when the large grain is thus oriented. Both of these cases are shown, along with the experimental results, in Fig. 3. It can be

seen that the concept of a very small nucleus triggering a portion of the main body of the sample fits the data best.

A further question that might be raised is whether it should not be the total internal field H_i, consisting of the vector sum of the local internal field H_ℓ and the applied field H_n, whose angular dependence should be considered rather than that of H_n alone. However, if H_i varies as $1/\cos\theta$, so will H_n, since whatever H_ℓ may be, its orientation relative to the sample remains the same.

2. Temperature Dependence of Coercive Force and Nucleating Fields in Cobalt-Rare-Earth Particles (J. J. Becker)

It is generally agreed that the coercive forces of the high-crystal-anisotropy cobalt-rare-earth intermetallic compounds, in particular the Co_5R class, are determined by the nucleation and motion of magnetic domain boundaries. These highly structure-sensitive processes are controlled by the number and nature of the imperfections present in the material. Thus the basis of the understanding and future development of this class of materials is the identification of these imperfections and the elucidation of their properties.

One approach to this problem is to study the way in which the intrinsic coercive force H_c depends on various physical parameters. Rather than the coercive force of bulk samples, one can study directly the fields H_n at which magnetization jumps have been found to occur in single particles.[1-4] It has already been found[5] that in Co_5Sm the dependence of H_c on the previous magnetizing field H_m is very strong, even when H_m is far larger than H_c. This behavior is also a property of individual particles, in which H_n is observed to take on various quantized values as H_m is varied.[1]

One can keep H_m constant and vary another parameter, the angle θ to the alignment direction of the sample. For a bulk sample, even if the constituent particle is considered to have a $1/\cos\theta$ dependence of H_c, the overall coercive force can show a maximum at 0°, or a minimum, or a maximum at intermediate angles, depending on the value of H_m.[10] In single particles, if H_m is kept constant and always applied at 0°, the angular variation of H_n can then show a very good $1/\cos\theta$ dependence,[11] as described in the previous section. In other cases it may not, or a single particle may show more than one jump, each with a different angular behavior.

A number of types of imperfections can be envisaged,[11] including purely geometrical effects, lattice deformations, composition variations, orientation variations, and combinations of these. In the attempt to deduce their nature from magnetic measurements, one of the most important parameters at one's disposal is the temperature, as the magnetic behavior of different types of imperfections should vary in quite different ways with temperature.

Some investigations of the temperature dependence of H_c of powders or sintered magnets have been reported. Velge and Buschow[12] investigated the dependence between room T and liquid nitrogen of a series of (La, Nd)Co_5 powders. McCurrie and Carswell[13] found a linear variation of H_c and also of H_r, the zero-remanence coercive force, with T in the same temperature range for Co_5Sm powders. The data of Martin and Benz[14] on sintered Co_5Sm magnets appear to fit a $T^{1/2}$ dependence best. In the data of Velge and Buschow,[12] the H_c of $NdCo_5$ powders varies in a way that is qualitatively consistent with the known variation of K with temperature.[15, 16] However, the reported variations of H_c of Co_5Sm with T[13, 14] are much greater than the variation of K or K/M_s with T reported by Tatsumoto et al.[16] In fact, they show a broad peak in K_1 for Co_5Sm at about 180°K, while the measurements referred to above show H_c strongly and monotonically increasing as the temperature goes down to 77°K. It thus appears that H_c is determined by something other than the bulk properties of Co_5Sm. Indeed, consistent with the idea that imperfections control H_c, the temperature dependence would be that of the imperfections themselves and would give some clue as to their nature.

Two experiments related to this problem are described here. It is again emphasized that H_c is a strong function of H_m. This dependence is shown in Fig. 4. Some Co_5Sm particles were prepared by lightly grinding a cast ingot and sizing to -250 +325 mesh (-61 +43μ) by the method of magnetic sieving.[1] Aggregates of particles were aligned in paraffin and measured in a vibrating-sample magnetometer. At room T, H_c nearly doubles as H_m goes from 20 to 44 kOe, even though H_c is only on the order of 0.05 H_m. At 77°K, the dependence is even more extreme. At H_m = 44 kOe, H_c is rising practically proportionally to H_m. Evidently the H_c values for a given H_m are several times as large as they are at room T. However, there is a conceptual difficulty in such a comparison. At first glance it might appear that we are observing that the relevant properties of remagnetization nuclei change rapidly with T. However, this implies that a given H_m at low T is equivalent to the same H_m at high T. But, whatever the details of the model may be, the significance of H_m depends in some way on its magnitude relative to the material constants. Whatever H_m does to the details of the domain structure depends on the properties of the material, including those of the imperfections, at the relevant T. It is not obvious in a case like this what two numbers should be compared at two temperatures, unless perhaps H_c is clearly approaching some limiting value with increasing H_m. This is more nearly the case in Fig. 5, which shows the behavior of particles prepared like those in Fig. 4 but with their surfaces smoothed in a chemical polishing solution.[1] Comparing this sample to the ground particles, the dependence of H_c on H_m is different at each T, the actual H_c levels are different, and their relative changes with T are not the same.

One way out of the dilemma presented by measurements on multiparticle samples is to follow individual magnetization jumps in single particles.

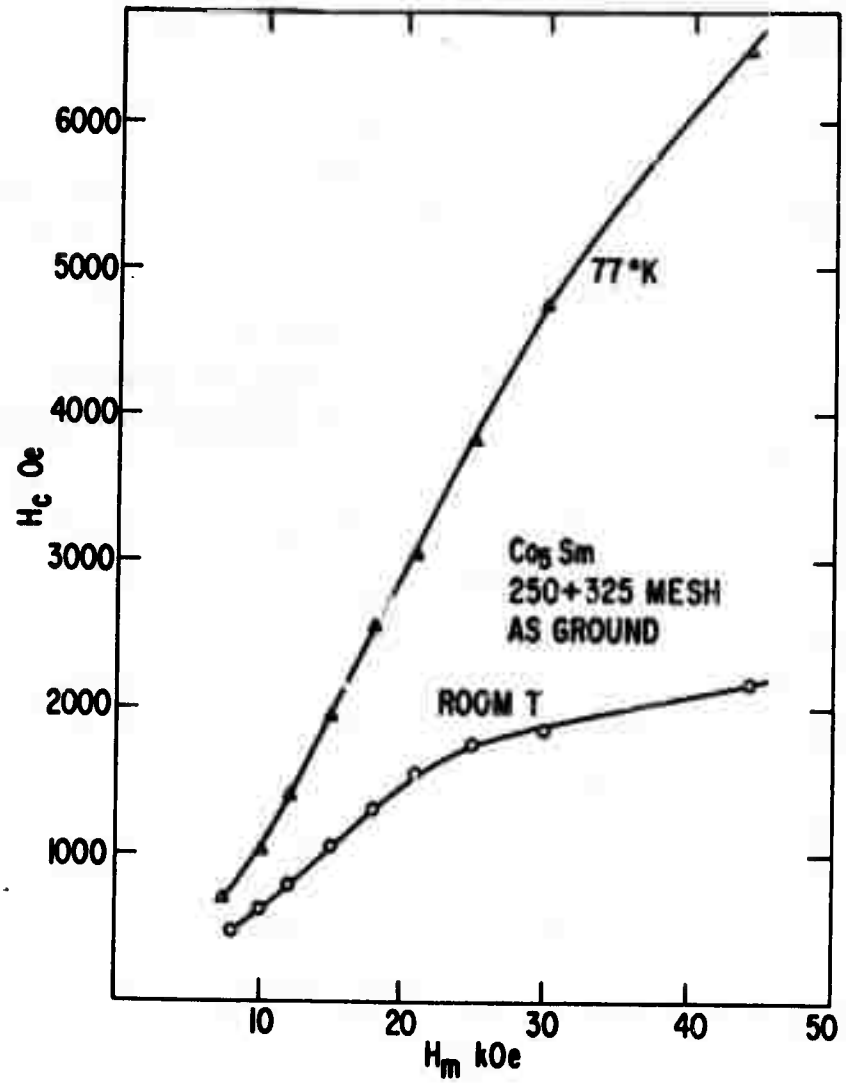

Figure 4 Dependence of coercive force H_c on magnetizing field H_m for ground and chemically polished Co_5Sm powder at room temperature and 77°K.

Typical behavior of a single particle is shown in Fig. 6. A given magnetization jump persists over a range of H_m, and if the temperature is gradually changed, the H_n for a given jump can be followed, with some confidence that the same physical event is being observed as a function of temperature. The sample studied showed a behavior similar to Fig. 6, with two jumps on each side of the loop, except that both were symmetrical. Presumably, then, only two nuclei were active. In Fig. 7 are shown the H_n observed as the temperature was gradually changed, H_m having always the value of 21 kOe and applied at the temperature of measurement. At high temperatures,

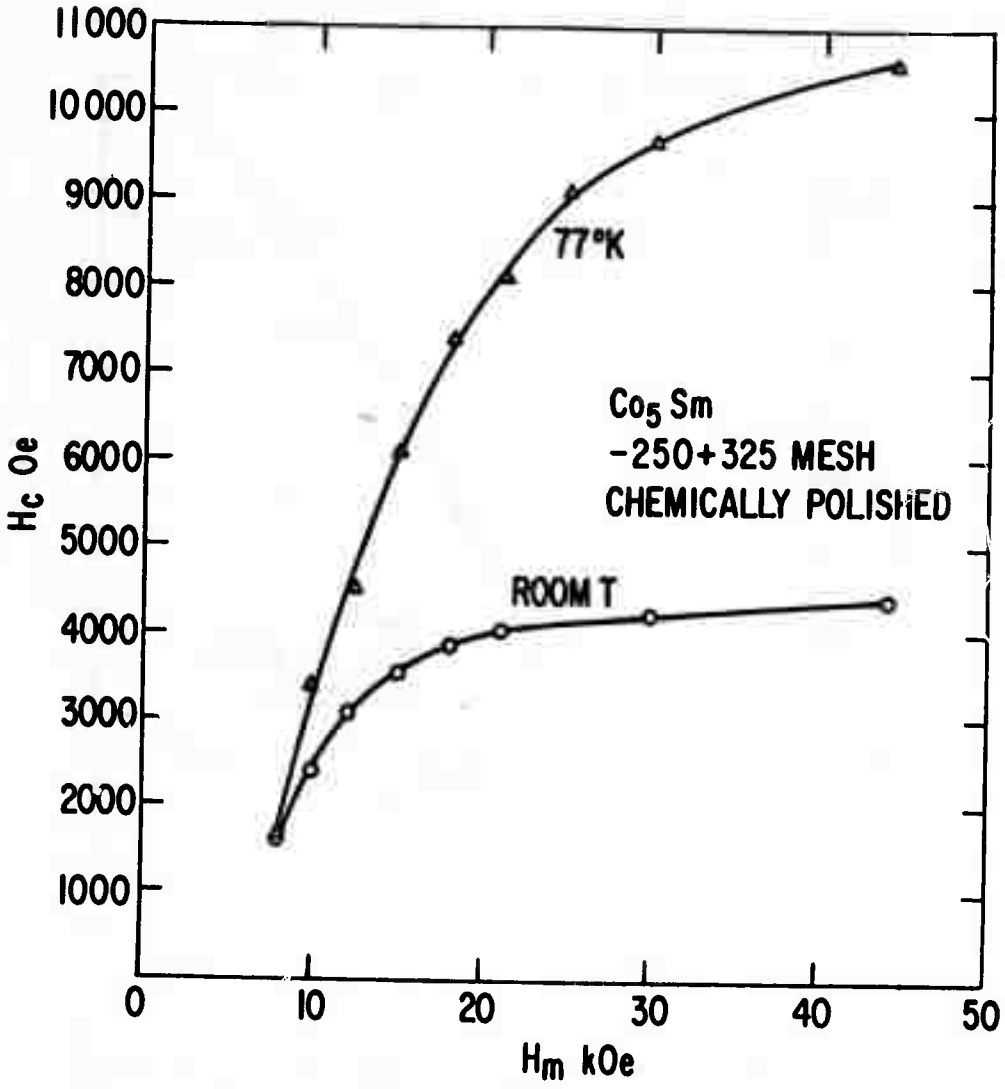

Figure 5 Dependence of coercive force H_c on magnetizing field H_m for ground and chemically polished Co_5Sm powder at room temperature and 77°K.

each pair of points corresponds to a symmetrical jump on opposite sides of the loop. As the temperature is lowered, the H_n for both jumps increase rapidly, but the one with the initially lower H_n rises more rapidly with decreasing T and overtakes the other at about -60°C. Below this temperature, the hysteresis loop is rectangular, the entire reversal being accomplished in one jump.

Several comments can be made on these results:

1) The variation of H_n with T is very large. H_n here is plotted as applied field. Whether and how much it should be modified to take account

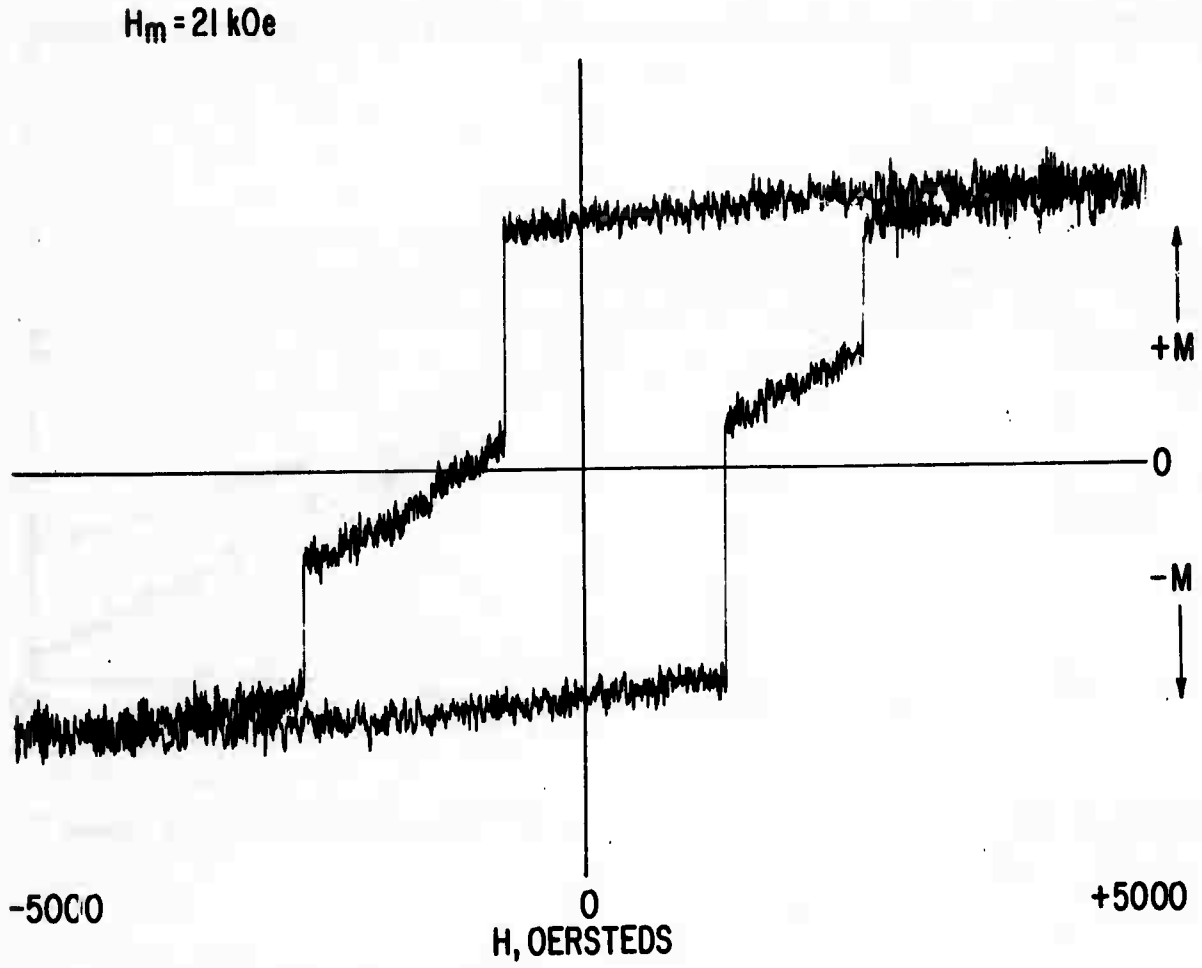

Figure 6 Hysteresis behavior of Co_5Sm single particle.

of internal demagnetizing effects is not entirely obvious. However, jumps do sometimes take place in positive H_n (same direction as H_m) so some internal field effects must be present. At worst these might be on the order of $4\pi M_s/3$, so that the true H_n in Fig. 7 would still vary by more than a factor of two in the temperature range shown. In any case H_n varies much more rapidly with T than the reported values of K or M or plausible combinations of them.

2) Two jumps in the same sample show different T dependences of H_n. This certainly suggests that two nuclei of different nature are responsible for them.

3) Since these jumps can be individually followed with slowly changing temperature, H_m is in some sense the same and we are observing the temperature dependence of the reversal process for a fixed initial condition.

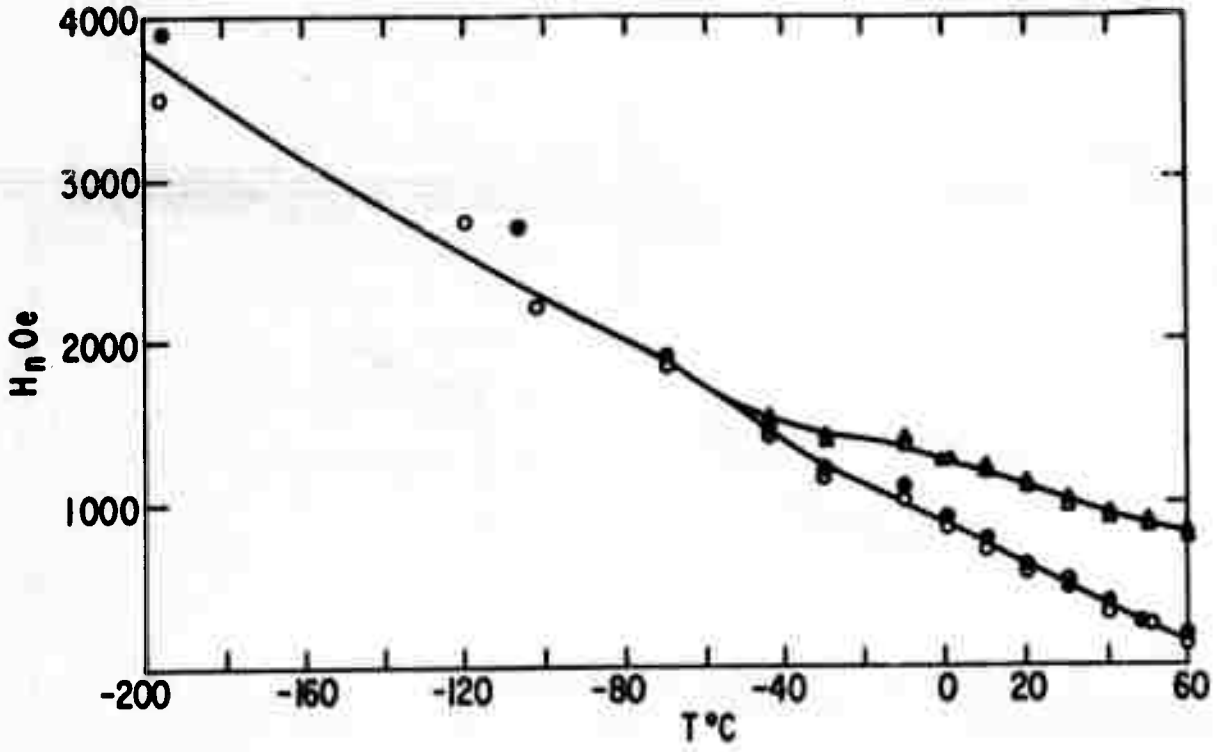

Figure 7 Temperature variation of H_n for individual magnetization jumps in Co_5Sm single particle.

4) The temperature dependence is monotonic, and like the H_c measurements on larger samples, shows nothing suggesting the peak in K at ~180°K reported by Tatsumoto et al.[16] However, it should be pointed out that there is a considerable amount of discrepancy between their values and those reported elsewhere. Strnat[17] gives a room T anisotropy field for Co_5Sm of about 235 kOe. The T variation he shows does not extend to the range of temperatures where the peak shown by Tatsumoto et al. occurs. Buschow and Velge[18] give 290 kOe for a single crystal, while the value of Tatsumoto et al. is about 400 kOe. Their value of K for Co_5Y agrees with Hoffer and Strnat's single-crystal measurements at room T[19] although the latter show somewhat more variation with T.[20] Tatsumoto's values for $NdCo_5$ are similar in their T variation to earlier measurements on powders[15] but an order of magnitude larger in value. It is to be hoped that further corroborative measurements of K in these materials will be forthcoming.

The question might finally be raised whether the T variation can be attributed to thermal activation over an energy barrier, as suggested by McCurrie.[21] Order-of-magnitude arguments suggest that this is unlikely. The simplest case is that of an isolated particle of volume V reversing thermally against K, which involves essentially comparing the orders of

magnitude of KV and kT. At room T for Co_5Sm, V is on the order of 10^{-22} cm^3, many orders of magnitude smaller than the particles present. If a region is considered to reverse within a larger particle, an additional large exchange energy makes the process, essentially thermally driven wall nucleation, impossible.[22] For the motion of a wall already present, K can be replaced by something of the order of M_sH_c, making V something like 10^{-19} cm^3, or an area of a wall only a few lattice constants in each dimension. The T dependence of H_c calculated for the Egami wall[23] comes only from the T dependence of the anisotropy constant K_6^6.

In conclusion, it appears that the T variation of both H_c in powders and sintered magnets and H_n in single particles is much more rapid than, and functionally different from reported values of the T variation of K for Co_5Sm. This appears to indicate that magnetization reversal is not controlled by the properties of pure Co_5Sm, but by those of the magnetization reversal nuclei present.

3. Magnet Domain Structure Studies and Transmission Electron Microscopy (J. D. Livingston)

Domain studies employing the Kerr effect have included estimation of the domain wall energy in Co_5Sm, qualitative observations of domain structures in various Co_5R, $Co_{17}R_2$, and Co_7R_2 castings, and studies of magnetization reversal in sintered magnets.

The coercive force of cobalt-rare-earth magnets is believed to be determined by the nucleation and/or pinning of domain walls. Thus the domain wall energy is a parameter of great fundamental importance, and it would be useful to have estimates of this quantity for the various cobalt-rare-earth compounds. Such estimates can be obtained from measurements of domain width in thin samples, for which the domain structures and related theoretical analyses are much simpler than for bulk samples.

A sample consisting of several large crystals of Co_5Sm was mounted and polished. Observation of the domain structure revealed that one of the large grains had a domain pattern typical of a crystal with the c-axis nearly normal to the surface. The sample was then thinned by polishing the opposite face, and the domain structure in this crystal was photographed at various sample thicknesses (Fig. 8). As sample thickness decreased, the complex corrugations and spike domains typical of bulk samples gradually disappeared, eventually becoming a simple maze structure (Fig. 8c). Specimen thickness was measured metallographically on a section polished perpendicular to the surface on which the domains were photographed. At a thickness of approximately 20μ, the average domain width was 3μ (Fig. 8c). Assuming this domain width to be the equilibrium width at this sample thickness, we estimate from standard theory that the domain wall energy in Co_5Sm is approximately 50 ergs/cm^2. This value should be considered tentative until we

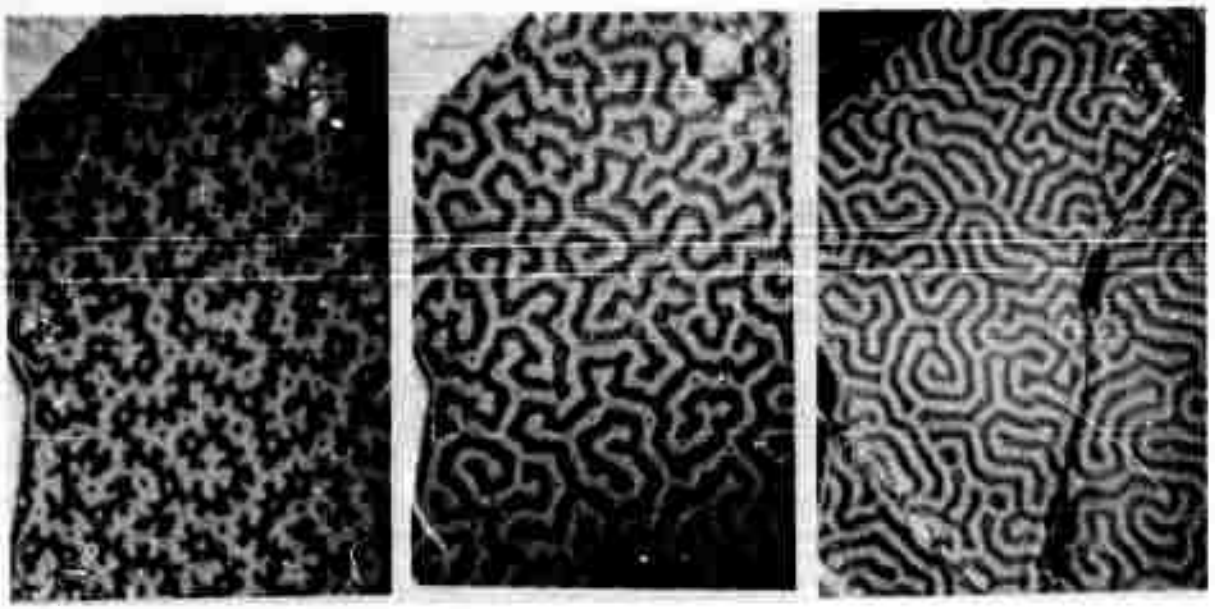

(a) (b) (c)

Figure 8 Change of domain pattern as thickness of Co_5Sm sample is decreased. Sample thickness: a, 70μ; b, 40μ; c, 20μ. 394X. 394X.

complete an improved version of this experiment, which is currently under way. We also plan to extend the technique to other cobalt-rare earth compounds.

In preparation for more quantitative studies of the type described above, qualitative observations were made of domain structures in various Co_5R, $Co_{17}R_2$, and Co_7R_2 castings. Domain patterns in Co_5Pr, Co_5Ce, and Co_5Y were characteristic of easy-axis magnetic anisotropy, but structures were generally finer than in Co_5Sm, suggesting that domain wall energies are lower in these compounds than in Co_5Sm (see Figs. 9, 10, and 11).

Domain patterns in $Co_{17}Sm_2$ were also of the easy-axis type, and finer than in Co_5Sm (Fig. 12). (A similar observation, comparing domain widths of $Co_{17}Sm_2$ and Co_5Sm grains in a sintered magnet, was included in our first semiannual report.) We were unable to detect magnetic domains in $Co_{17}Pr_2$ and $Co_{17}Y_2$, and saw only faint lamellar domains in $Co_{17}Ce_2$. We tentatively conclude that these compounds have easy-plane magnetic anisotropy. Domains in $Co_{17}Gd_2$ were complex, but some grains showed patterns suggestive of easy-axis anisotropy (Fig. 13).

Recent studies of Ray and Strnat have indicated that although most $Fe_{17}R_2$ and $Co_{17}R_2$ compounds are of the easy-plane type, several mixed $(Co, Fe)_{17}R_2$ compounds have easy-axis anisotropy. We have confirmed

Figure 9 Domains in Co_5Sm casting. 355X.

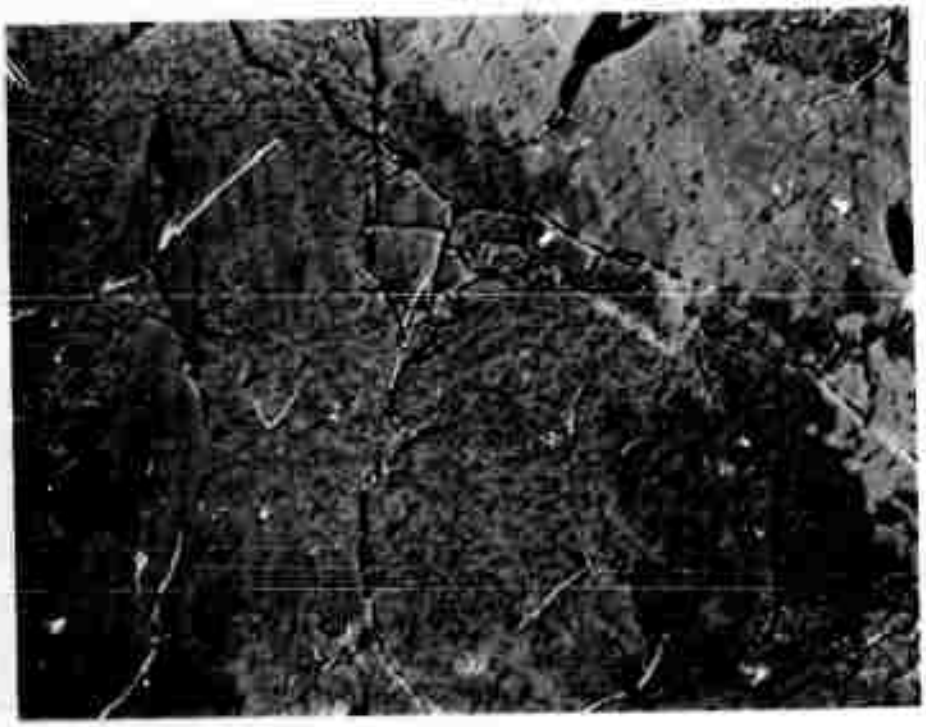

Figure 10 Domains in Co_5Pr casting. 370X.

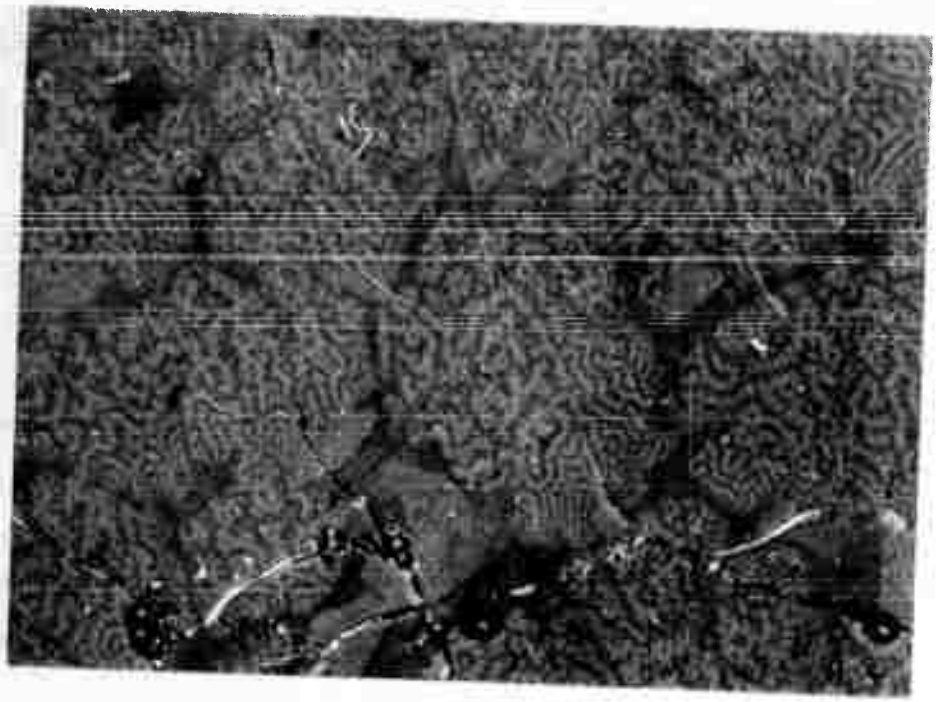

Figure 11 Domains in Co_5Ce casting. 370X.

Figure 12 Domains in $Co_{17}Sm_2$ casting. 375X.

Figure 13 Domains in $Co_{17}Gd_2$ casting. 89X.

these observations for several compounds, having observed easy-axis domain patterns in the following compounds:

$(Co_{0.9}Fe_{0.1})_{17}Sm_2$	(Fig. 14)
$(Co_{0.75}Fe_{0.25})_{17}Sm_2$	(Fig. 15)
$(Co_{0.7}Fe_{0.3})_{17}Gd_2$	(Fig. 16)
$(Co_{0.7}Fe_{0.3})_{17}Y_2$	(Fig. 17)
$(Co_{0.75}Fe_{0.25})_{17}Ce_2$	(Fig. 18)

Domain patterns in a Co_7Sm_2 casting were coarse and complex (Fig. 19), but were tentatively identified as non-equilibrium easy-axis patterns. Patterns in other Co_7R_2 compounds were generally finer and suggestive of easy-axis symmetry, but were complex because of a fine and irregular grain structure (e. g., Fig. 20). We expect to repeat these observations on samples annealed at high temperature.

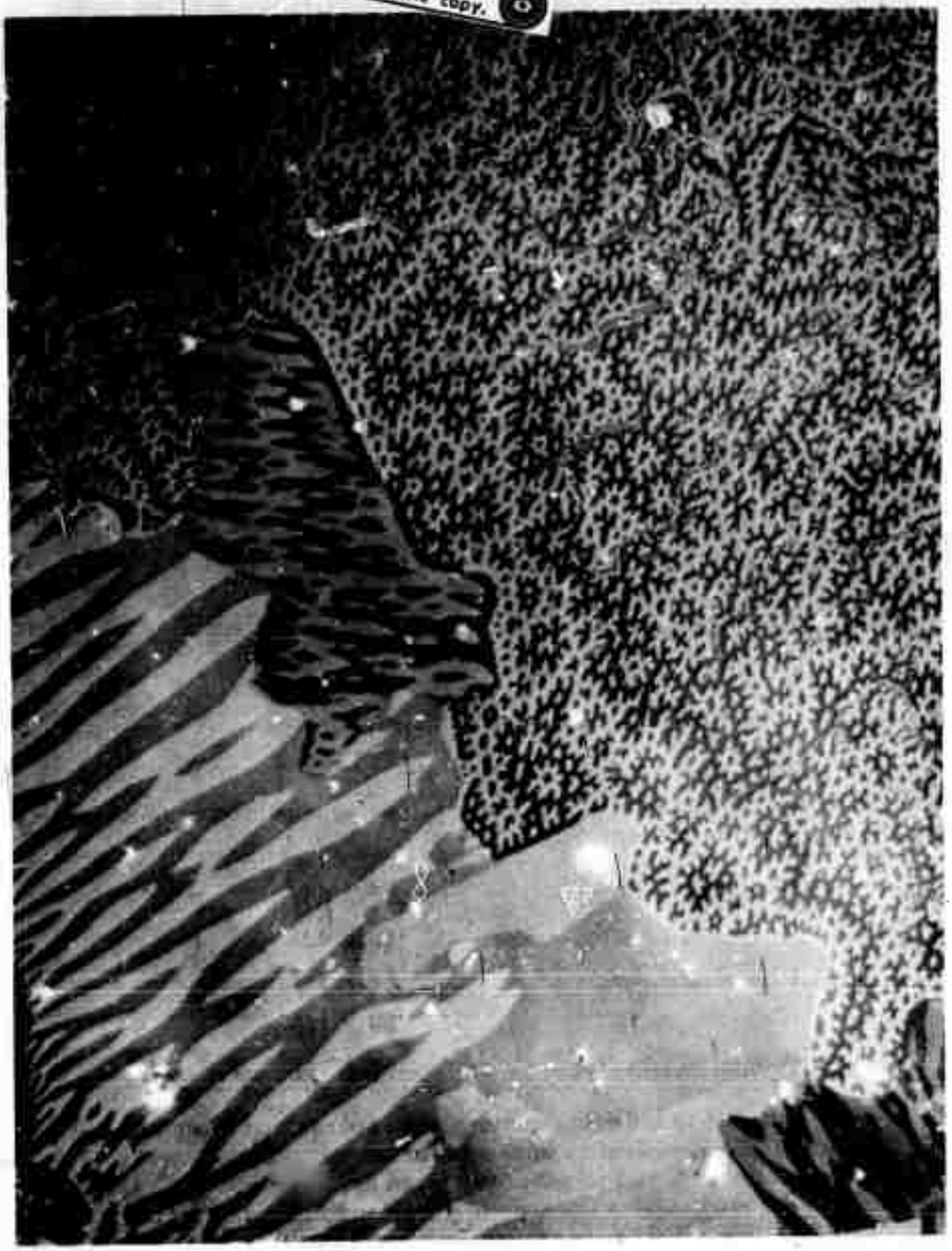

Figure 14 Domains in $(Co_{0.9}Fe_{0.1})_{17}Sm_2$ casting. 880X.

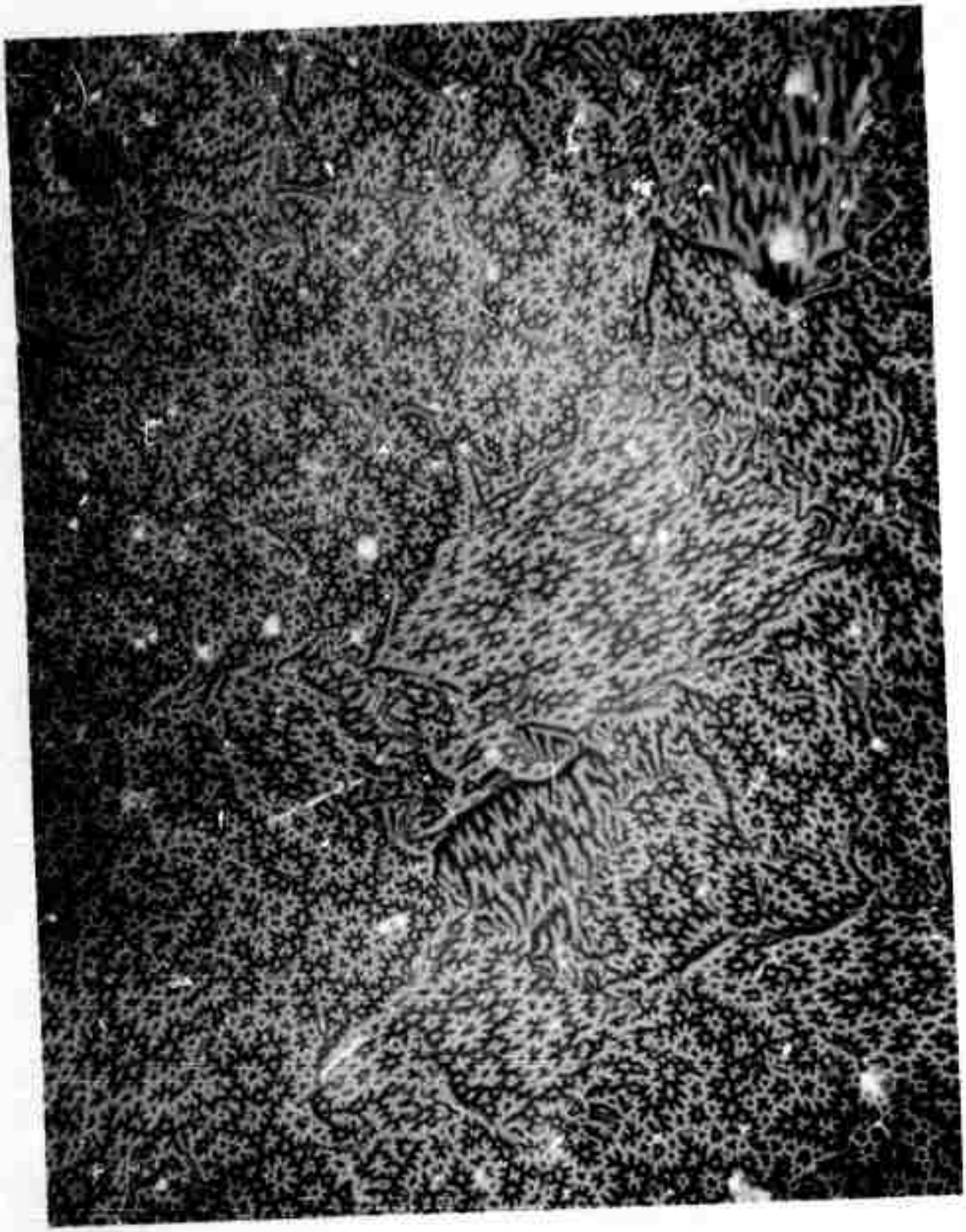

Figure 15 Domains in $(Co_{0.75}Fe_{0.25})_{17}Sm_2$ casting. 880X.

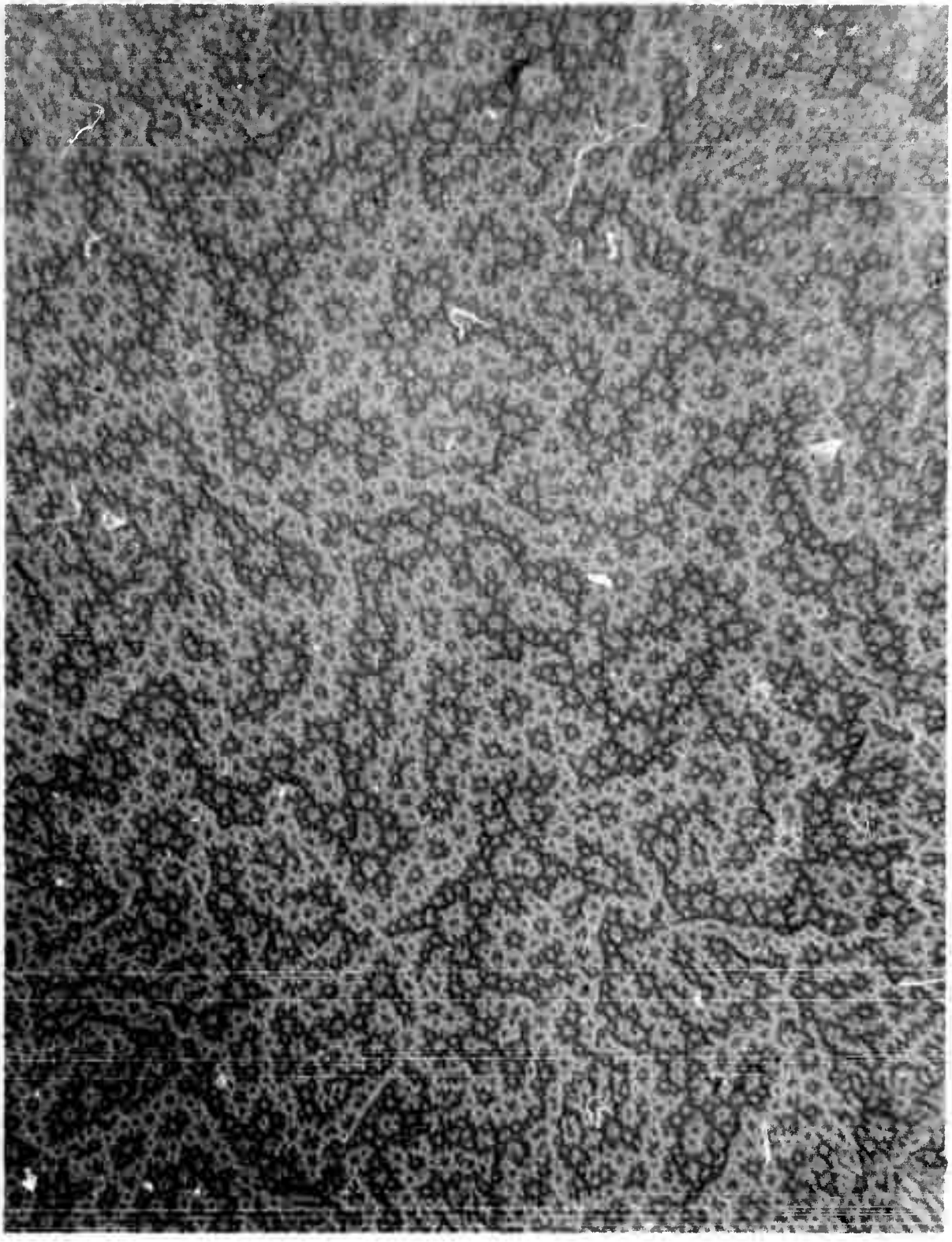

Figure 16 Domains in $(Co_{0.7}Fe_{0.3})_{17}Gd_2$ casting. 880X.

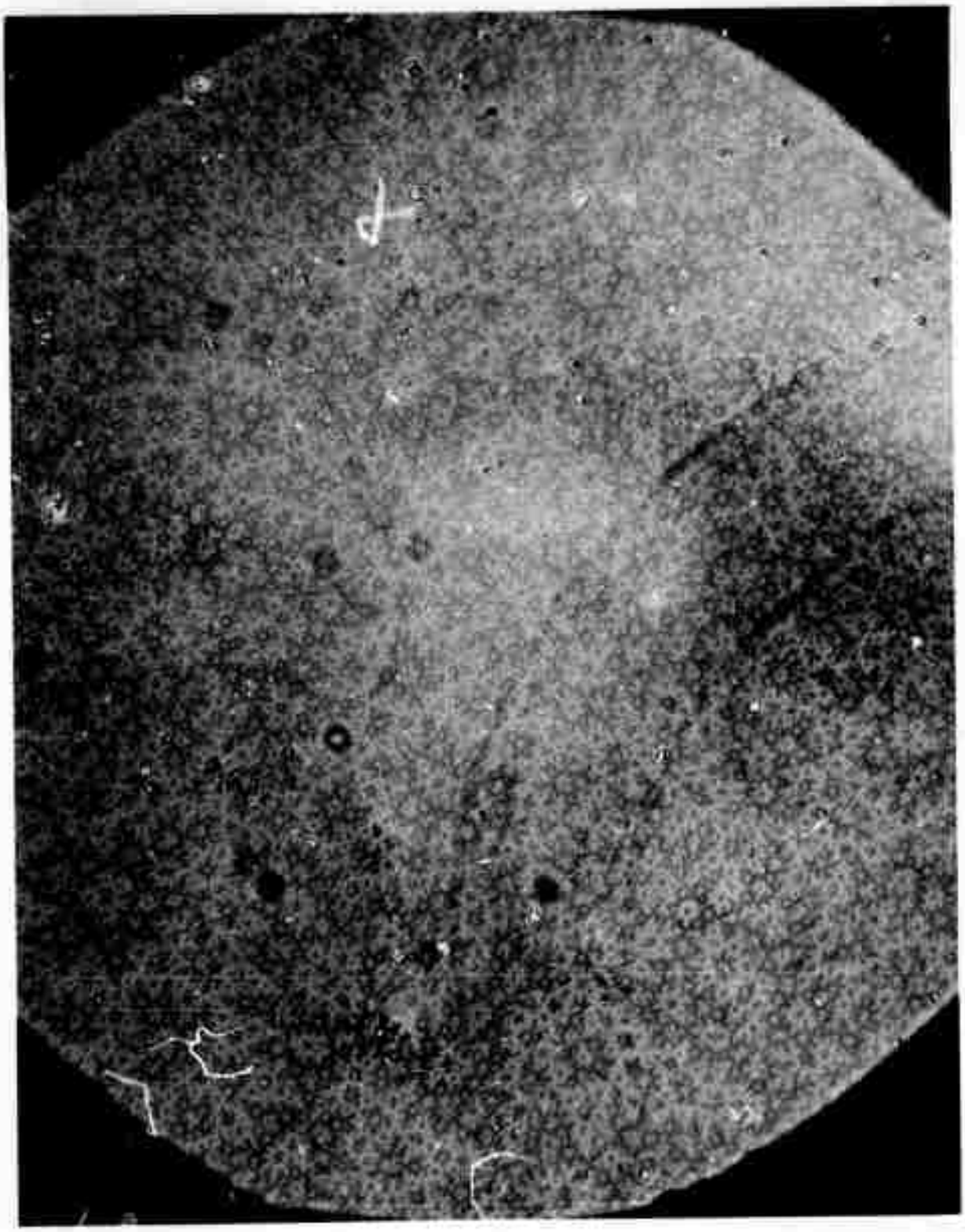

Figure 17 Domains in $(Co_{0.7}Fe_{0.3})_{17}Y_2$ casting. 880X.

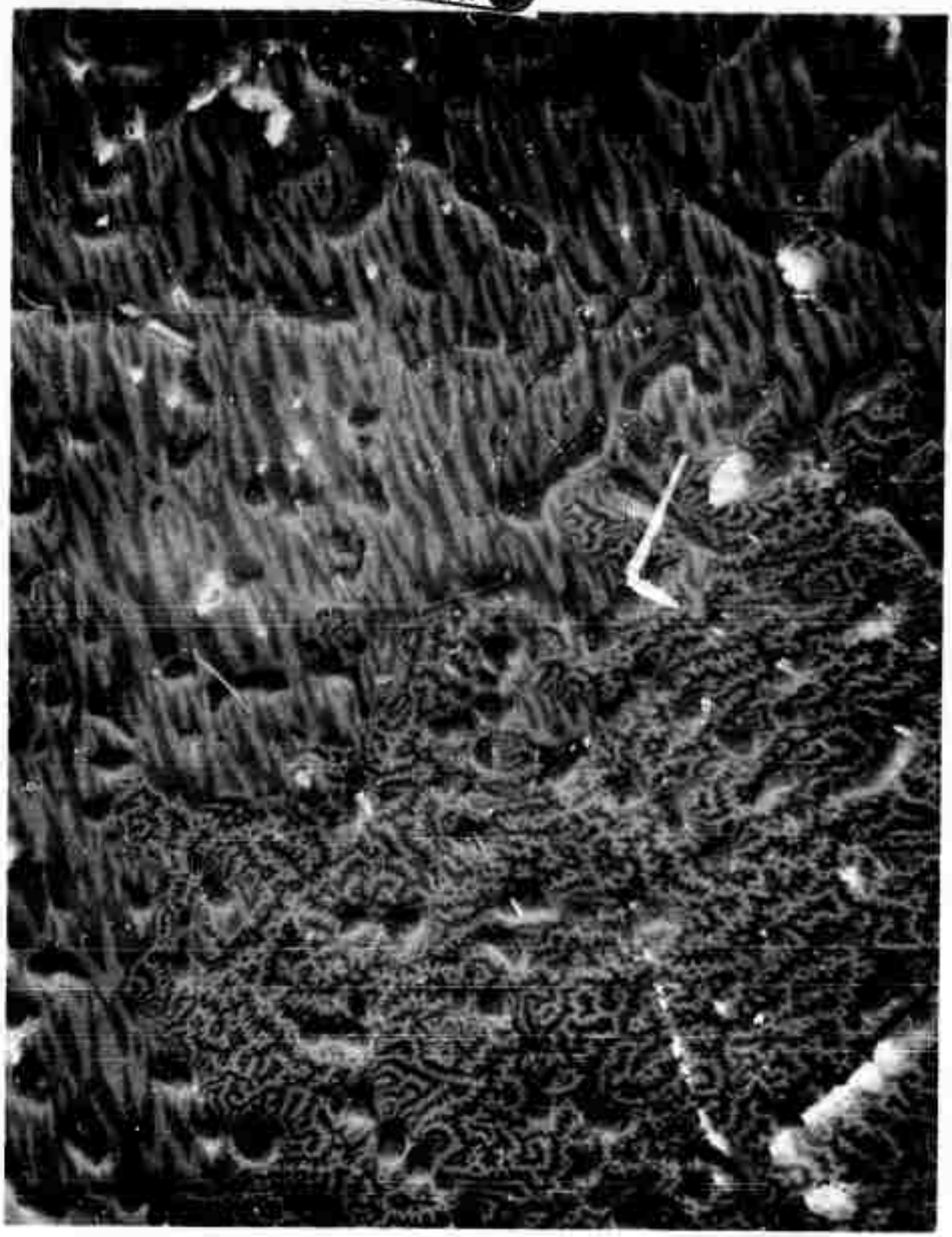

Figure 18 Domains in $(Co_{0.75}Fe_{0.25})_{17}Ce_2$ casting. 880X.

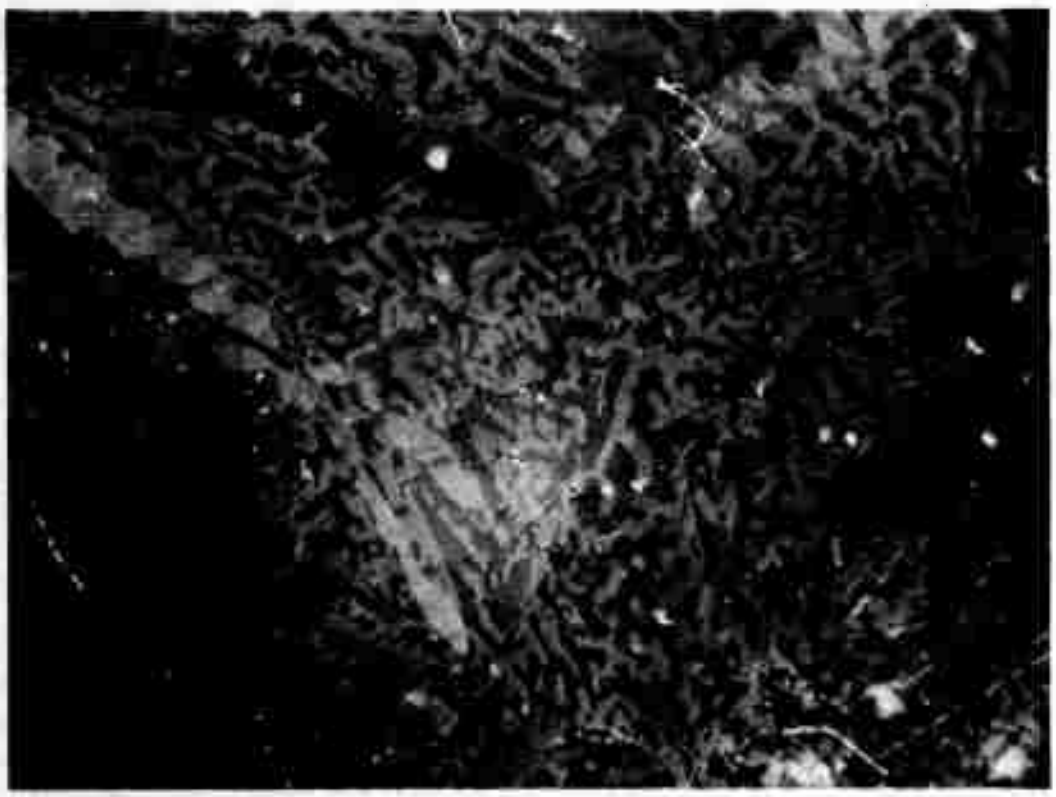

Figure 19 Domains in Co_7Sm_2 casting. 400X.

Figure 20 Domains in Co_7Pr_2 casting. 375X.

Studies of magnetization reversal in sintered Co-Sm magnets have continued, and will be described in a later report.

As part of a program to identify microstructural changes associated with the heat treatment of Co_5Sm, E. F. Koch of our Materials Characterization Operation has been developing techniques for transmission electron microscopy of this difficult material.

Slices 20 mils thick have been cut from Co_5Sm castings. These slices are then ground to 5 mils thickness, and then ion-thinned until a hole appears. Thinning Co_5Sm from 5 mils initial thickness requires over 100 hours of ion-thinning time, but attempts to grind to less than 5 mils thickness have been unsuccessful.

Insertion of the entire Co_5Sm sample into the electron microscope produces extreme disturbance of the electron beam by stray magnetic fields, and no pictures could be obtained. Instead, small bits of the sample were broken off near the hole and transferred to the microscope grid with vacuum tweezers. In some regions, edges of these bits are thin enough to be transparent to electrons, and transmission micrographs can be obtained. Structural features observed in an as-cast sample include individual dislocations (Fig. 21), dislocation networks (Fig. 22), and microtwins (Fig. 23). Full comparison of samples heat-treated at various temperatures has not yet been completed.

III. MATERIALS CHARACTERIZATION AND PHASE EQUILIBRIUM STUDIES

1. Comparison of Analytical Results (J. G. Smeggil)

A set of Co_5Sm materials prepared by liquid phase sintering with nominal compositions from 61.4 wt % Co to 64.2 wt % Co were cut into representative sections for wet analytical techniques and x-ray fluorescence spectroscopy. One member of the set to be done via wet chemical techniques was submitted to Ledoux. The other member of this set was given to D. H. Wilkins of our Materials Characterization Operation for in-house chemical analysis.

Figure 21 Transmission electron micrograph of Co_5Sm casting, showing numerous dislocations. 45,000X.

Figure 22 Transmission electron micrograph of Co_5Sm casting, showing dislocation network. 44,000X.

Figure 23 Transmission electron micrograph of Co_5Sm casting, showing a series of parallel microtwins. 106,250X.

The analytical data reported by Ledoux and Wilkins are listed below:

Sample No.	Wilkins % Sm	Wilkins % Co	Ledoux % Sm	Ledoux % Co
868-A	34.8	64.8	34.2	65.1
868-B	35.3	64.6	34.6	64.9
868-C	35.8	63.9	35.0	64.4
868-D	36.2	63.5	35.4	63.9
868-E	36.4	63.0	36.0	63.5
868-F	36.9	62.6	36.1	63.2
868-K	37.2	62.3	36.8	62.5
868-L	37.8	62.1	37.1	62.3

These data are also plotted in Fig. 24. Since the samples were prepared with uniform variations in composition from sample to sample, the sample number is plotted on the absicca and the wt % Co and wt % Sm along the ordinate. The appearance of Fig. 24 clearly shows that non-random errors are involved in one or both of the analytical techniques used to generate these data. Clearly this problem must be rectified before these data and the associated samples can be used as standards for an instrumental technique.

The set of samples to be used as standards for the instrumental technique are currently being used in some preliminary experiments to evaluate x-ray fluorescence spectroscopy as an applicable instrumental procedure for the analysis of these materials.

2. Rare Earth Substitutions (J. G. Smeggil)

Attempts have been made to substitute Ca, Ba, or Sr for the rare earth in the Co_5R phase. The technique used was to melt the Co under argon, add the appropriate alkaline earth, and then pour the melt into a cooled copper hearth as quickly as possible. Unfortunately no significant amount of any of these three elements appeared to dissolve in the Co metal. The net result of each attempt was essentially the production of an ingot of Co metal.

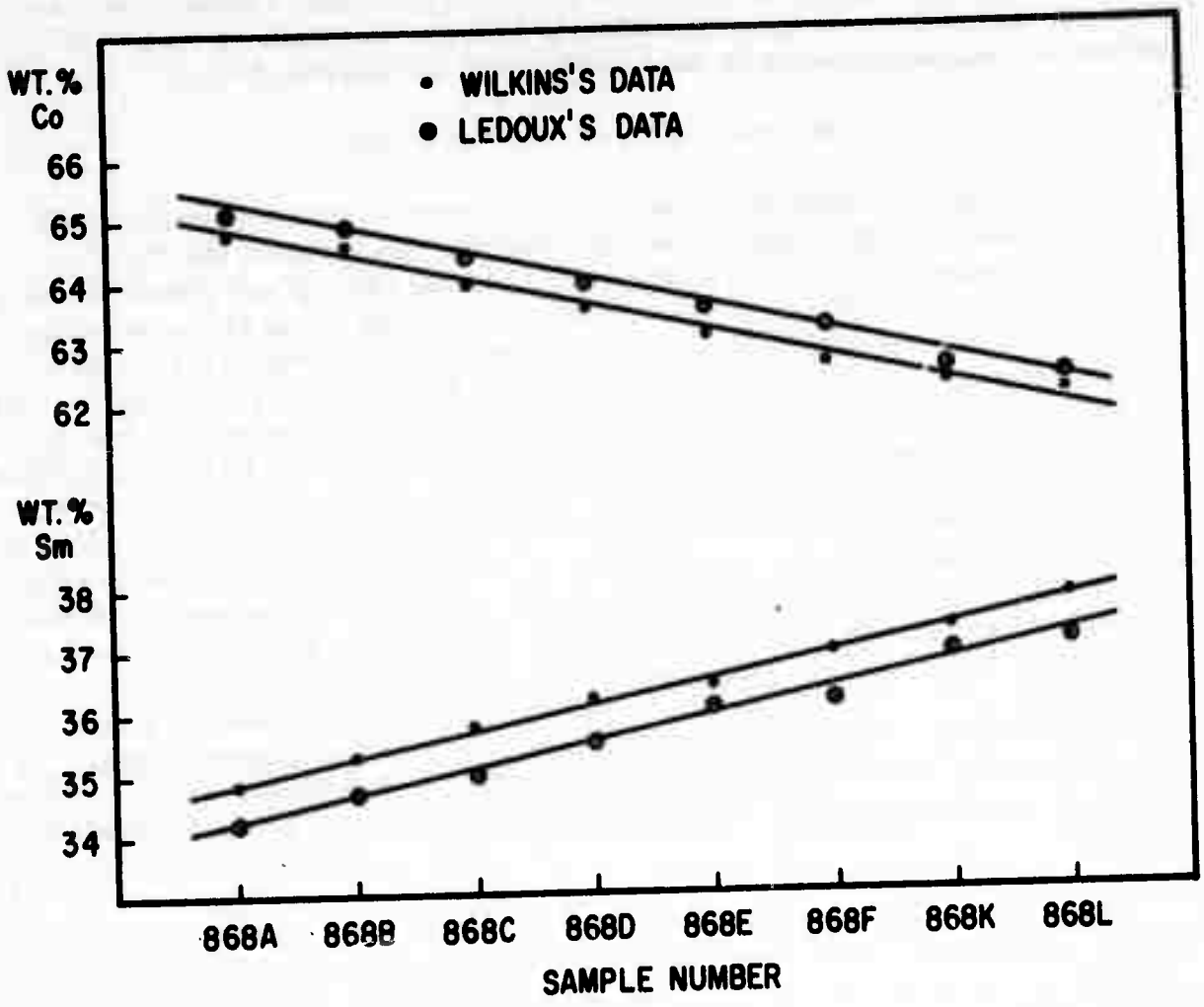

Figure 24 Comparison of analytical data from two sources on series of Co-Sm alloys.

IV. ALLOY DEVELOPMENT

1. A 10,000 Oe B-Coercive Force Magnet (R. J. Charles, D. L. Martin, L. Valentine, and R. E. Cech)

(The text of the following section is identical with that of a paper that has been submitted for publication in the A. I. P. Conference Proceedings.)

INTRODUCTION

Many previous researches[24-30] have illustrated that the production of high-energy, fine particle permanent magnets from transition metal-rare earth compounds depends upon careful control of interdependent processing parameters. The present work describes a series of high performance

cobalt-rare earth magnets for which sintering practice, composition, and heat treatment have been systematically adjusted to attain an optimum remanent magnetization with near theoretical B-coercive force.

EXPERIMENTAL PROCEDURES

Composition: Within the class of cobalt-rare earth compounds, Co_5R, with a single axis of magnetization the Co_5Pr phase exhibits the highest saturation value (≈1.2 tesla [12 kGauss]) and thus the highest potential energy product (BH_{max} ≈286 kJ/m^3 [36 MGOe]). † Utilizing liquid phase sintering (Ref. 27), Tsui and Strnat[30] have described an off-stoichiometry cobalt praseodymium magnet (61.8 w/o Co, balanc Pr) yielding an energy product of 127 kJ/m^3 [16 MGOe] or about 45% of the theoretical maximum for this composition. The B-coercive force, $\mu_0 H_c$[H_c] of 0.5 tesla [5 kOe] was about 59% of that theoretically attainable for the particular magnet described (i. e., 0.59 B_r). Martin and Benz[20] had previously shown that the substitution of half of the praseodymium by samarium at times yielded higher coercivities and consequently higher magnet properties. The particular specimen showing the highest energy product, 183 kJ/m^3 [23 MGOe], and remanent magnetization, 0.996 tesla [9.96 kGauss], was of the nominal composition 63 w/o Co, 13.6 w/o Pr, and 23.4 w/o Sm. It gave a B-coercive force ($\mu_0 H_c$) of 0.68 tesla or 69% of that attainable for this particular magnet. In the same study of Co-Pr-Sm alloys the maximum B-coercive force achieved was 0.88 tesla [8.8 kOe] or 99% of the limiting value set by the remanence, J_r.

Because of the higher over-all properties obtained with Co-Pr-Sm alloys, additional experimentation has been made on this system. In the current work the Pr/Sm weight ratio was increased to about 1.3 while the cobalt content was maintained at about 63 w/o. Alloy powders were prepared by blending a base powder containing the praseodymium with a 60% Sm - 40% Co additive. The additive was used to promote densification by a liquid phase sintering process.[27] The base material, containing about 67% Co, was prepared by direct reduction of praseodymium and samarium oxides in the presence of cobalt by calcium.[31] In order to assure that the resultant alloy powder consisted of individual grains of a sufficiently small size for magnet fabrication (≈10μ), the alloy was processed through a fluid energy mill.[32] Measurements of the J-coercive force of the alloy base powder gave the relatively low value of $\mu_0 H_c$ of about 0.15 tesla [1.5 kOe].

Magnet fabrication: The importance of maintaining high coercivity in a magnet structure has been previously indicated. Our experience indicates that it is often difficult to maintain high, reproducible coercivity in samples sintered to full density. In general, a small amount of porosity obtained by slightly "under sintering" is usually preferable. Such "under sintering" prevents a compact from undergoing exaggerated grain growth which may tend to diminish coercivity. Systematic study of temperatures and times

of sintering is necessary, therefore, to delineate optimum conditions for a given composition. This is particularly so in view of the fact that excessive porosity is deleterious to magnetization.

Successful sintering of near 5-1 compounds of cobalt-rare earths has been shown generally to require off-stoichiometry compositions (rare earth excess) of the final magnets.[27, 28, 33] Such off-stoichiometry will, to a first approximation, reduce the saturation magnetizations from stoichiometric values in direct proportion to the reduced cobalt contents of the final alloys. Such reductions must presently be tolerated, for only in this manner is it possible to achieve high coercivity simultaneous with high sintered density.

Test samples in this work were aligned and pressed to a packing density of about 80% by methods previously described.[27, 29, 32] After sintering all samples exhibited a packing fraction (p) greater than 0.9 of that for full density (8.5 g/cc) and an alignment factor ($A=J_r/J_s$) greater than 0.95.

RESULTS

Figure 25 shows data, typical for each of a number of blended Co-Pr-Sm compositions, from which an optimum sintering temperature can be determined for a given composition. The sintering times were fixed at one hour. The results shown include the sample of nominal composition 62.87% Co which exhibited the highest properties obtained in this investigation. Similar results were obtained for near neighbor compositions and indicate that satisfactory magnet properties can be achieved by sintering for one hour at a temperature between 1105° and 1120°C. Outside of this temperature-time range the properties decrease markedly. Figure 26 shows the demagnetization results for the sample of 62.87% Co which showed the highest magnet properties. The energy product is high (207 kJ/m^3 [26 MGOe]), but attention should be drawn to the fact that the B-coercive force exceeds 1.0 tesla [10 kOe] and that this value is about 99% of the limit set by the remanent magnetization.

Figure 27 illustrates the effect of composition on properties. In this case the points plotted correspond to the results obtained at an optimum sintering temperature for each composition. These optimum temperatures varied over the full range of sintering temperatures shown in Fig. 25 with the highest optimum sintering temperatures occurring for those compositions near 63 w/o Co.

It is important to note that the most desirable composition ranges shown in Fig. 27 are those in which $\mu_0 H_k$ exceeds the B-coercive force. * In such a case the demagnetization curve exhibits nearly ideal behavior and the low load line irreversible losses encountered at elevated temperature operation will, in general, tend to be minimized. The effect of sintering temperature on $\mu_0 H_k$ is further illustrated in Fig. 26 in which the J curves for various sintering temperatures are given. The temperature of 1120°C was the optimum

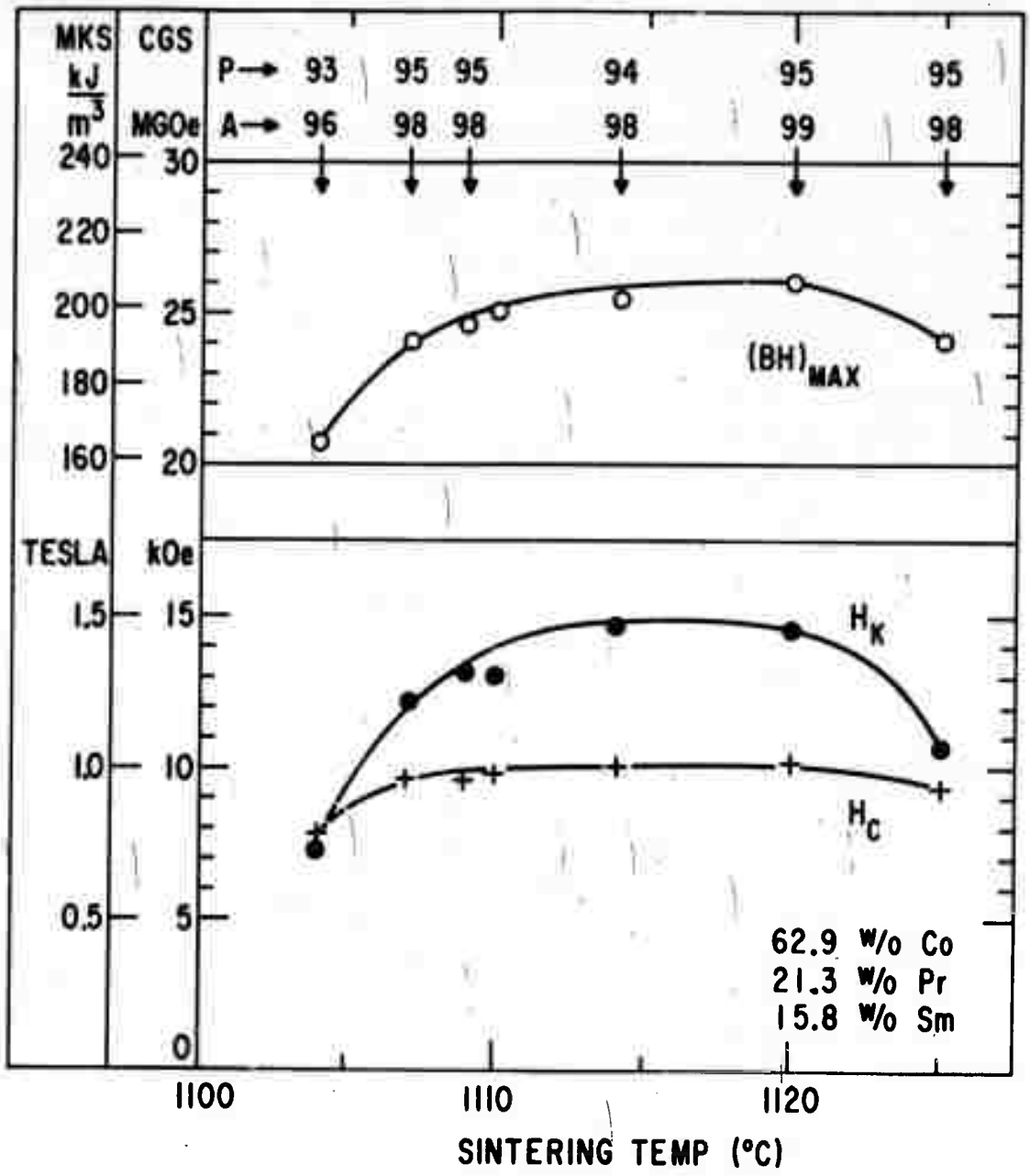

Figure 25 Variation of magnetic properties, packing (p), and alignment (A) with sintering temperature.

temperature. At sintering temperatures above and below 1120°C the properties decrease substantially. With reference to the numerical sample data given in Figs. 25 and 27, it is clear that the exceptional properties of the sample in Fig. 26 result from a high alignment factor (A), an adequate packing fraction (p), and a sufficiently high $\mu_0 H_k$ to allow nearly ideal B-coercive force.

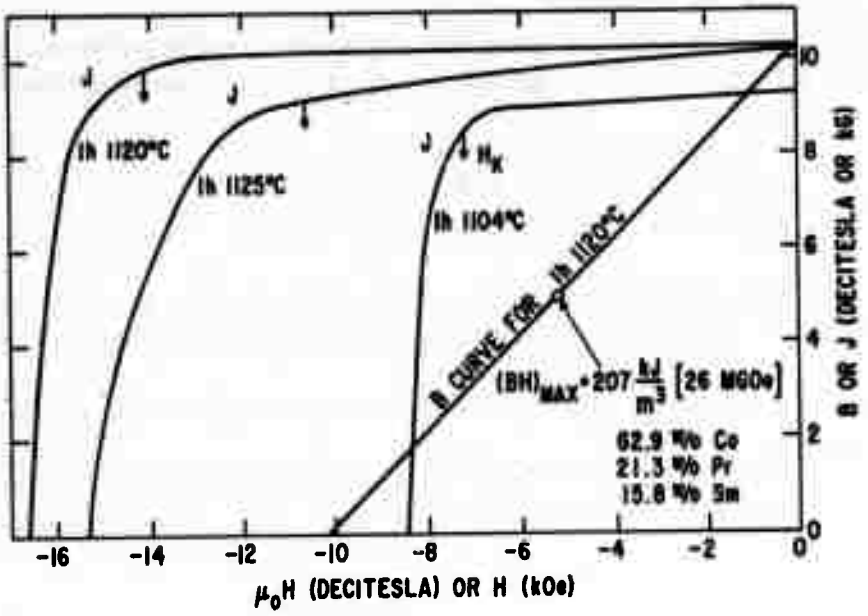

Figure 26 Changes in the J-demagnetization curve with sintering temperature. The B-demagnetization curve for the 1120°C sample is also given.

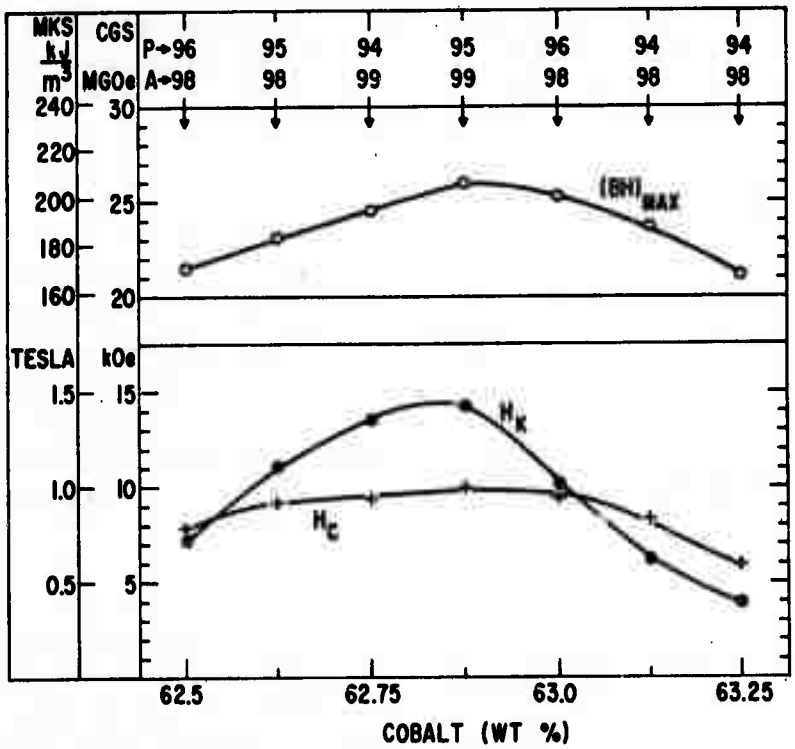

Figure 27 Variation of magnetic properties, packing (p), and alignment (A) with composition for a series of Co-Pr-Sm alloys sintered in the range 1105° to 1125°C. The peak value for each composition is listed.

SUMMARY

By optimization of composition and sintering heat treatment, the following properties of a Co-Pr-Sm permanent magnet have been achieved:

J_r = 1.026 tesla [10.26 kG)
$\mu_0 H_c$ = 1.013 tesla [10.13 kOe]
$(BH)_{max}$ = 206.9 kJ/m^3 [26.0 MGOe]

It has also been shown that the magnetic properties of such magnets are highly sensitive to variations in composition and sintering temperature.

2. Sintering of Cobalt-Rare-Earth Permanent Magnets (M. G. Benz and D. L. Martin)

(The text of the following section is identical with that of a paper that has been submitted for publication in the A. I. P. Conference Proceedings.)

INTRODUCTION

Several combinations of one or more of the rare earths have been used to fabricate sintered cobalt-rare earth permanent magnets.[25, 27-30, 33-37] These combinations generally include one or more of the rare earth elements La, Ce, Pr, Nd, and Sm. In an effort to simplify this discussion, work considered in this report will be limited to the Co_5Sm system. Since the rare earths are a close-knit family of elements, Co_5Sm serves well as a model for what is observed in the other systems.

PROCESS

The process sequence used to fabricate high performance cobalt-rare earth permanent magnets usually consists of: (1) alloy preparation by melting and casting, (2) comminution of the cast alloy to a fine powder (particle size approximately 10 μM. At this stage each powder grain is essentially a single crystal), (3) magnetic alignment of the powder grains (c-axis parallel to the direction of the applied field), (4) densification by application of pressure followed by high temperature diffusion type sintering, (5) post sintering thermal treatment to optimize coercivity, and (6) magnetization.

OXYGEN

Oxygen is a factor in this process, as it is in most powder metallurgy type processes. The oxygen content of the magnets fabricated for this study varied between 0.3 and 0.7 wt %, as determined by vacuum fusion analysis. These are large values for metallic systems, and hence the source and location of the oxygen must be carefully considered.

During melting, vacuum melting practices are used to reduce the dissolved oxygen level in the cobalt prior to addition of the rare earth metal. The rare earth metal is added to the deoxidized cobalt under an inert atmosphere, and a further reduction in the dissolved oxygen level occurs by oxidation of a very small portion of the rare earth. This rare earth oxide forms a slag which is left behind in the crucible during the casting process. Little is known about the solubility of oxygen in bulk castings. They are too difficult to sample directly without introduction of additional oxygen by the sampling process itself. One can estimate, however, that the oxygen content of the casting is much less than 0.01 wt %.

Next the casting is crushed. At -20 mesh, analytical samples can be readily taken and show 0.03 to 0.05 wt % oxygen for a Co + 34 wt % Sm alloy. This increase in oxygen level is considered to result from the increased surface area and hence the volume of surface oxide.

As the crushed alloys are pulverized and finally milled to smaller diameters, the surface area increases and the surface oxide layer formed on these fresh surfaces represent a greater fraction of the total. At the 10 μM particle size for powder milled in nitrogen but subsequently handled in air, one measures 0.3 to 0.7 wt % oxygen. This is a tenfold increase over the oxygen content for the -20 mesh sample, and indicates that most of the oxygen in the system at this stage exists as a oxide layer coating the surface of each powder grain.

During magnetic alignment no change is noted in the oxygen level.

During the first stage of densification by pressing, no change in the oxygen level is observed. A surface oxide layer is still considered to exist on each crystal grain in the pressed compact.

During the final stage of densification by sintering, again no change in the total oxygen level is observed, but a significant change in the location of this oxygen does occur. After sintering, the oxide layers no longer coat each grain. Furthermore, small oxide particles (diameter $<<1$ μM) are not left behind at the grain boundaries. At least they have not been observed along the grain boundaries using electron microscopy of replicas of fractured surfaces. What is observed, however, are large crystals (size approximately 1 μM) located in the pores which exist at multigrain corners. These are clearly observed using scanning electron microscopy to view a fractured surface. Use of an x-ray scan of such an area shows a change in the Sm peak to Co peak ratio from 0.85 for the bulk grain to 3.0 for the pore area. This strongly suggests that the pore area is rich in samarium, and we postulate that this is due to the presence of samarium oxide in the pore.

COMPOSITION

On the basis of the above, the sintered alloy will be considered to exist as a mixture of one or more Co-Sm metal phases with an oxide phase. The oxide phase will be considered to be Sm_2O_3. Furthermore, it will be assumed that the oxygen solubility in the Co-Sm metal phases is so small that for a first approximation all of the oxygen measured for a particular sintered sample will be assumed to be present as part of the oxide phase. Hence the composition of the Co-Sm metal phases must be adjusted to take into account the Sm that went to make up the Sm_2O_3. For example, a sample containing 62.1 wt % Co, 37.5 wt % Sm, and 0.4 wt % oxygen would be assumed to consist of 2.77 wt % oxide phase and 97.23 wt % Co-Sm metal phases. Hence, the Co-Sm metal phases would have an average composition of 64.1 wt % Co and 35.9 wt % Sm instead of 62.1 wt % Co and 37.5 wt % Sm that exist for the total system.

COMPOSITION AND SINTERING

In order to determine what influence composition might have on sintering and magnetic properties, a series of four alloys was prepared with nominal compositions varying from Co + 34 wt % Sm to Co + 37 wt % Sm. Powders with an average particle size of 5.4 μM were prepared from these alloys. Samples were prepared from each powder by magnetic alignment at 60 kOe, hydrostatic pressing with 200 kpsi to a density of 6.88 g/cm^3 (relative density = 0.8), sintering at 1120°C for 1 hour, age cooling at a rate of approximately 1°C/min to 900°C, and chamber cooling to room temperature. At this point, shrinkage $\Delta V/V_0$ was calculated from the measured change in density and the intrinsic coercive force was measured after magnetization at 60 kOe. These results are listed in Table I. Remarkable increases in $\Delta V/V_0$ and H_{c_i} are noted for the sample from powder lot A as compared to the samples from powder lots B through D. Analysis of lots A and B for Co, Sm and oxygen, and adjustment of the compositions of the metal Co-Sm phases as outlined in the preceding section, showed that lot A has an adjusted composition of 34.5 wt % Sm and lot B has an adjusted composition of 32.9 wt % Sm. On an atomic % basis, precise stoichiometry for Co_5Sm occurs at 16.66 at % Sm. Deviations from this composition will be noted by the symbol δ_{Sm}. When δ_{Sm} is positive, the alloy will be referred to as hyperstoichiometric. When δ_{Sm} is negative, the alloy will be referred to as substoichiometric. As noted in Table I, samples from lots A and B have adjusted compositions on the Co-Sm metal phases which bracket the stoichiometric composition of 16.6 atom % Sm. Furthermore, the remarkable increase in shrinkage and the dramatic increase in intrinsic coercive force occur as the composition goes from substoichiometric.

TABLE I

Powder Lot:	D	C	B	A
Nominal Composition				
Sm, wt %	34	35	36	37
Co, wt %	66	65	64	63
After Sintering				
$\Delta V/V_0$	0.069	0.086	0.090	0.167
H_{c_i}, kOe	-6.0	-4.1	-2.4	-17.5
Analytical Composition				
Sm, wt %			35.6	36.8
Co, wt %			63.4	62.5
O, wt %			0.64	0.56
Phases				
Sm_2O_3, wt %			4.4	3.9
Co-Sm, wt %			95.6	96.1
In Co-Sm Phases				
Sm, wt %			32.9	34.5
Sm, at %			16.1	17.1
δ_{Sm}, at % Sm			-0.5	+0.5

BLENDING

From the preceding section it would appear that the final composition of the sintered alloy must be hyperstoichiometric with regard to the Co-Sm metal phases. In order to achieve this, one must control not only the Sm content of the alloy but also the oxygen content of the powder. Rather than attempt to control this delicate balance at the melt stage, we have used blending of powders of different compositions to achieve the desired final composition. In this way the Co, Sm, and O content of each powder is established by the original melt compositions and the state of surface oxidation of the powder. This in turn is determined by the particle size and shape. By blending two such powders, one is able to achieve a hyperstoichoimetric Co-Sm metal phase in the sintered alloy. As noted in Tables II and III, the same remarkable increases in shrinkage and H_{c_i} are noted for the blend cases at a nominal 36 to 37 wt % Sm final composition. These studies were done without precise analysis, but as the oxygen levels will be somewhat similar to the direct melt study discussed in the previous section, one can again draw the conclusion that hyperstoichiometric compositions after

TABLE II

Shrinkage $\Delta V/V_0$

Wt %, Sm (Nominal)									
		Blend							
Base	Add	32	35	35.5	36	36.5	37	37.5	38
25	60	0.097							0.135
32	43					0.116	0.162	0.167	0.172
34	41		0.039	0.059	0.143	0.143			
34	50			0.067	0.121	0.154	0.146		
34	60			0.073	0.112	0.144	0.154		
36	37				0.089	0.158	0.167		

TABLE III

Intrinsic Coercive Force, H_{c_i} kOe

Wt %, Sm (Nominal)									
		Blend							
Base	Add	32	35	35.5	36	36.5	37	37.5	38
25	60	-1.8							-45.4*
32	43					-9.7	-14.3	-13.0	-11.1
34	41		-3.5	-2.6	-15.8	-13.7			
34	50			-2.1	-9.9	-12.4	-11.1		
34	60			-2.0	-9.9	-11.3	-9.9		
36	37				-2.4	-19.2	-17.5		

*Sample not aligned.

adjustment for oxygen are essential in order to achieve rapid shrinkage and a high intrinsic coercive force.

SUMMARY

Using Co_5Sm as a model cobalt-rare earth permanent magnet system, this report includes a discussion of: (1) the process sequence used to fabricate

high performance cobalt-rare earth permanent magnets, (2) the role of oxygen in this process, (3) the adjustment of composition necessary to account for the oxide present, (4) observations relating shrinkage during sintering and intrinsic coercive force to deviations from stoichiometry, and (5) the use of blending for composition control.

For: (1) observations of time and temperature effects during sintering, (2) a model to explain the shrinkage observations, and (3) several reasons that might explain why a high intrinsic coercive force is observed for hyper-stoichiometric compositions, the reader is referred to Ref. 38.

REFERENCES

1. J. J. Becker, IEEE Trans. Magnetics MAG-5, 211 (1969).
2. J.J. Becker, J. Appl. Phys. 42, 1537 (1971).
3. H. Zijlstra, J. Appl. Phys. 42, 1510 (1971).
4. J.J. Becker, IEEE Trans. Magnetics MAG-7, 644 (1971).
5. J.J. Becker, J. Appl. Phys. 39, 1270 (1968).
6. J.J. van den Broek and H. Zijlstra, IEEE Trans. Magnetics MAG-7, 226 (1971).
7. K. Bachmann, IEEE Trans. Magnetics MAG-7, 647 (1971).
8. J.J. Becker, J. Appl. Phys. 41, 1005 (1970).
9. S. Reich, S. Shtrikman, and D. Treves, J. Appl. Phys. 36, 140 (1965).
10. J.J. Becker, J. Appl. Phys. 38, 1015 (1967).
11. J.J. Becker, 17th Conference on Magnetism and Magnetic Materials, Chicago, Nov. 1971.
12. W. A. J. J. Velge and K. H. J. Buschow, IEEE Conference on Magnetic Materials and Their Applications, London, Sept. 1967.
13. R. A. McCurrie and G. P. Carswell, Phil. Mag. 23, 333 (1971).
14. D. L. Martin and M. G. Benz, IEEE Intermag. Conference, 1972.
15. H. Bartholin, B. van Laar, R. Lemaire, and J. Schweitzer, J. Phys. Chem. Solids 27, 1287 (1966).

16. E. Tatsumoto, T. Okamoto, H. Fujii, and C. Inoue, J. de Phys. 32, C1-550 (1971).

17. K. J. Strnat, IEEE Trans. Magnetics MAG-6, 182 (1970).

18. K. H. J. Buschow and W. A. J. J. Velge, Z. angew. Phys. 26, 157 (1969).

19. G. Hoffer and K. Strnat, IEEE Trans. Magnetics MAG-2, 487 (1966).

20. G. Hoffer and K. Strnat, J. Appl. Phys. 38, 1377 (1967).

21. R. A. McCurrie, Phil. Mag. 22, 1013 (1970).

22. A. Aharoni, J. Appl. Phys. 33, 1324 (1962).

23. T. Egami, 17th Conference on Magnetism and Magnetic Materials, Chicago, Nov. 1971.

24. K. H. J. Buschow, W. Luiten, P. A. Naastepad, and F. F. Westendorp, Philips Tech. Rev. 29, 336 (1968).

25. D. K. Das, IEEE Trans. Magnetics MAG-5, 214 (1969).

26. K. H. J. Buschow, P. A. Naastepad, and F. F. Westendorp, J. Appl. Phys. 40, 4029 (1969).

27. M. G. Benz and D. L. Martin, Appl. Phys. Let. 17, 176 (1970).

28. R. E. Cech, J. Appl. Phys. 41, 5247 (1970).

29. D. L. Martin and M. G. Benz, Cobalt 50, 11 (1971).

30. J. Tsui and K. Strnat, Appl. Phys. Let. 18, 107 (1971).

31. R. E. Cech, unpublished.

32. M. G. Benz et al., Tech. Rept. AFML-TR-71-142, Air Force Materials Lab., Wright-Patterson Air Force Base, Ohio.

33. D. K. Das, IEEE Trans. Magnetics MAG-7, 432 (1971).

34. J. Tsui, K. Strnat, and R. Harmer, J. Appl. Phys. 42, 1539 (1971).

35. M. G. Benz and D. L. Martin, J. Appl. Phys. 42, 2786 (1971).

36. D. L. Martin and M. G. Benz, IEEE Trans. Magnetics MAG-7, 291 (1971).

37. R. J. Charles, D. L. Martin, L. Valentine, and R. E. Cech, 17th Conference on Magnetism and Magnetic Materials, Chicago, Nov. 1971.

38. M. G. Benz and D. L. Martin, submitted to J. Appl. Phys.